

# Advances in MEMS and Microfluidics-Based Energy Harvesting Technologies

M. A. Parvez Mahmud, Sajad Razavi Bazaz, Soroush Dabiri, Ali Abouei Mehrizi, Mohsen Asadnia, Majid Ebrahimi Warkiani,\* and Zhong Lin Wang\*

Energy harvesting from mechanical vibrations, thermal gradients, electromagnetic radiations, and solar radiations has experienced rapid progress in recent times not only to develop an alternative power source that can replace conventional batteries to energize portable and personal electronics smartly but also to achieve sustainable self-sufficient micro/nanosystems. Utilizing micro-electromechanical system (MEMS) and microfluidics technologies through selective designs and fabrications effectively, those energy harvesters can be considerably downsized while ensuring a stable, portable, and consistent power supply. Although ambient energy sources such as solar radiation are harvested for decades, recent developments have enabled ambient vibrations, electromagnetic radiation, and heat to be harvested wirelessly, independently, and sustainably. Developments in the field of microfluidics have also led to the design and fabrication of novel energy harvesting devices. This paper reviews the recent advancements in energy harvesting technologies such as piezoelectric, electromagnetic, electrostatic, thermoelectric, radio frequency, and solar to drive self-powered portable electronics. Moreover, the potential application of MEMS and microfluidics as well as MEMS-based structures and fabrication techniques for energy harvesting are summarized and presented. Finally, a few crucial challenges affecting the performance of energy harvesters are addressed.

harvesters that can replace conventional energy sources.<sup>[1]</sup> Microelectronic devices use small rechargeable or nonrechargeable batteries as their primary source of power. However, these batteries have a limited and uncertain lifetime, have difficulty replacing, and hence maintenance intensive. Energy harvesting devices are becoming an increasingly viable solution and may one day replace conventional batteries in low power applications.<sup>[2]</sup>

Microfluidics analysis is one of the important research fields in MEMS, exhibiting broad market prospects due to characteristics, e.g., flexibility and the ability of rapid thermal transport.<sup>[3]</sup> Microfluidic devices are remarkably flexible and can be stretched in shape and size, allowing them to convert the deformation of the material into electricity.<sup>[4]</sup> It makes them capable of integrating the MEMS-based energy harvesters in self-powered sensors<sup>[5]</sup> located in various environments, such as the human body.<sup>[6]</sup> Also, microfluidics technology can be used for increasing

the performance efficiency of energy harvesters by using as a heat exchanger<sup>[7]</sup> or embedding in the housing system.<sup>[8]</sup> Also, MEMS technology, which allows microscale structures to be fabricated inside energy harvesting devices, has enormously improved harvesting methods. It is a microstructure that ensures physical interactions happen in a tiny space so that the size of the harvester can be minimized and energy density can be improved.

## 1. Introduction

Energy harvesting is capturing energy from the ambient environment and converting it into usable electric power. Recent advances in low-energy electronics have increased the need for sustainable, portable, and reliable energy source. The significant growth in micro-electromechanical systems (MEMS) technology has given rise to the development of various energy

M. A. P. Mahmud  
School of Engineering  
Deakin University  
Geelong, Victoria 3216, Australia  
S. R. Bazaz, M. E. Warkiani  
School of Biomedical Engineering  
University of Technology Sydney  
Sydney, NSW 2007, Australia  
E-mail: majid.warkiani@uts.edu.au  
S. Dabiri  
Institute for Environmental Engineering  
University of Innsbruck  
Innsbruck 6020, Austria

A. A. Mehrizi  
Biomedical Engineering Division  
Department of Life Science Engineering  
Faculty of New Sciences and Technologies  
University of Tehran  
Tehran 1417935840, Iran  
M. Asadnia  
School of Engineering  
Macquarie University  
Sydney, NSW 2109, Australia  
Z. L. Wang  
School of Material Science and Engineering  
Georgia Institute of Technology  
Atlanta, GA 30332-0245, USA  
E-mail: zlwang@gatech.edu

 The ORCID identification number(s) for the author(s) of this article can be found under <https://doi.org/10.1002/admt.202101347>.

DOI: 10.1002/admt.202101347

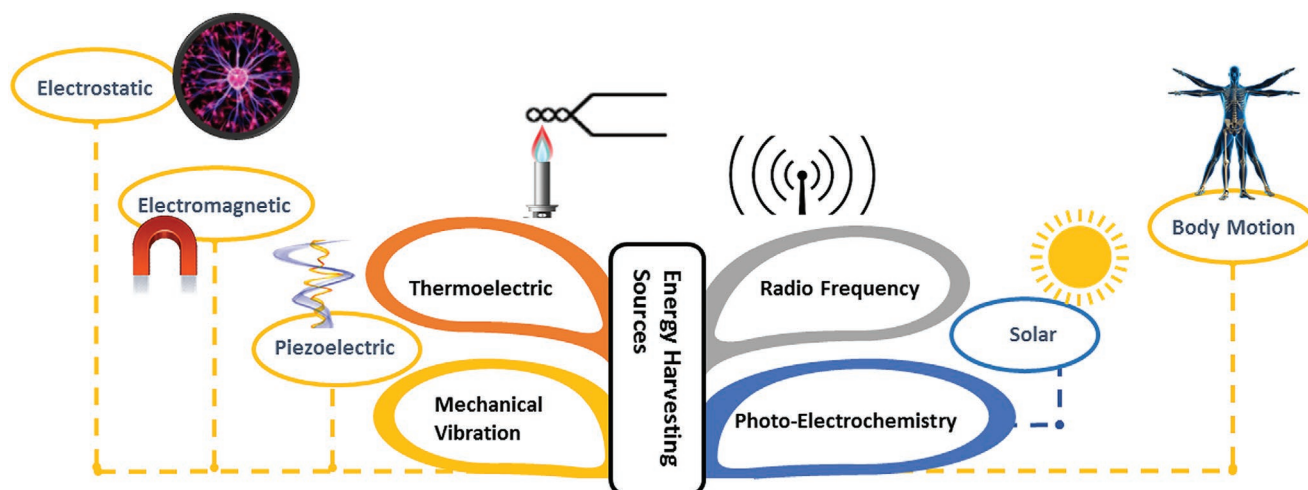


**Figure 1.** Main sources for MEMS and microfluidics-based energy harvesting, categorized in nine groups.

This research summarizes the main methods of harvesting residual energy from the environment in order to discuss the research performed in these areas. As outlined in **Figure 1**, the overall topic of energy harvesting can be broken down into seven sections: piezoelectric, electromagnetic, electrostatic, thermoelectric, radio frequency, solar, and kinetics. These energy harvesting methods are among the most effective and widely used and have significantly impacted the developments in the MEMS and microfluidic industries. Each section will include an overview of the mechanism behind the energy harvesting technique, the main design and structures, fabrication procedures, as well as a discussion on the current and future applications. This is the first review paper covering energy harvesting technologies such as piezoelectric, electromagnetic, electrostatic, thermoelectric, radio frequency, and solar to drive self-powered portable electronics, review their analytical performance, and highlight critical shortcomings yet to be resolved. The review is significant as it analyses and demonstrates the future development roadmap of MEMS and microfluidics technologies for energy harvesting.

## 2. Mechanical Vibration-Based Energy Harvesting

Mechanical vibration energy can be a valuable power source of energy harvesting system. Machine vibration mostly comes from common sources. Thus, frequency and strength are relatively low. **Table 1**<sup>[9]</sup> shows different vibration sources' essential vibration sources, including natural frequency and corresponding accelerated speed. MEMS energy harvesting is an alternative that primarily involved scavenging energy from natural resources, thereby reducing the consumption of exhaustible forms of energy. By implementing MEMS technology for energy harvesting, we would have a free energy source that requires less maintenance and can potentially last for a lifetime.<sup>[10]</sup> As shown in **Table 1**, the fixed frequency of the vibration source is relatively low, around 80–300 Hz.<sup>[9]</sup> Therefore, the study on vibration energy harvester must combine some vibration sources in some particular working environments.

To convert mechanical vibration into electricity, three kinds of transduction mechanisms are established: piezoelectric, electromagnetic, and electrostatic.<sup>[11]</sup> The main form of piezoelectric energy harvesting is to collect strain energy of piezoelectric materials, and displacements of electromagnetic coils generate electricity. As for electromagnetic, an AC voltage is generated across the coil, due to the change in the magnetic flux caused by the relation motion between the magnetic mass and the coil. For electrostatic, there is a current flow in the external circuit as a result of the vibration of a movable electrode. Based on these methods, energy harvester can provide electrical applications with a long service time.<sup>[12]</sup> In this part, these three kinds of MEMS vibration energy harvesting devices are discussed.

### 2.1. Piezoelectric Energy Harvesting

Piezoelectric energy harvesting technology uses the piezoelectric effect and transfers mechanical energy into electrical energy.<sup>[13]</sup> This technology is used in various structures, e.g., bulk, thin film, and nanowires.<sup>[14]</sup> In this system, the energy collection has high density, can avoid electromagnetic and heat interference, and produce large voltage with the transformer. Also, it is easy to process and realize integration and minia-

**Table 1.** Natural frequency and acceleration magnitude of vibration sources from the ambient environment.<sup>[9]</sup>

Vibration sources	Acceleration magnitude [m s <sup>-2</sup> ]	Natural frequency [Hz]
Car engine	12	200
Kitchen blender	6.4	121
Closing door or window	3	125
Microwave oven	2.5	121
Window near busy road	0.7	100
Foot traffic on wooden board walk	1.3	385
Bread machine	1.03	121
Washing machine	0.5	109

turization. Therefore, it is suitable for all kinds of sensors and monitoring systems.

Certain solid materials, such as crystals, certain ceramics, and some polymers that generate an electric charge are exposed to mechanical stress. This phenomenon is called piezoelectricity, and certain solid materials with this property are called piezoelectric materials. Piezoelectric material provides us with a new way of energy supply for MEMS devices. Also, MEMS technology has provided an advanced method of fabricating energy harvesting devices.<sup>[15]</sup>

The recent research works in piezoelectric energy harvesting technology is mainly focused on the characteristics of the piezoelectric ceramic materials and the influence of the power generation factors. These theoretical studies have solved the problem of piezoelectric ceramic materials in practical applications such as motion sensors, watches, ultrasonic power transducers, lithotripters, ultrasonic cleaning, ultrasonic welding, and active vibration dampeners,<sup>[16]</sup> but the characteristics of piezopolymers have been of interest to the researchers as well.<sup>[17]</sup> Also, some studies are analyzing the energy conversion efficiency in piezoelectric materials.<sup>[18–20]</sup> For instance, Song et al.,<sup>[19]</sup> to achieve high energy conversion efficiency, presented a spiral cantilever structure, where the piezoelectric lead zirconate titanate (PZT) thin film, which was 1.8 μm in thickness, was deposited on a platinized silicon-on-insulator (SOI) wafer. The maximum output power of 23.3 nW was obtained in the five turns spiral MEMS harvester excited at 0.25 g and at its resonance frequency of 68 Hz.

In early 1984, American scientists Hausler and Stein<sup>[21]</sup> put a PVDF sheet in organisms based on the energy produced by the rib stretching motion when the organism breathed. Then, they converted the energy into electricity to drive external equipment. The piezoelectric energy harvesting device was fixed on the dog ribs, and the dog's natural breathing could produce 18 V with voltage energy of 17 μW. Also, as shown in refs. [22,23], energy storage and energy transfer circuits have been of interest to researchers. The piezoelectric energy collection field's main research direction and development trend are focused on researching the low power consumption circuit design and highly efficient storage circuit.

In 2002, Sodano<sup>[24]</sup> stored the power generated by bending deformation of the piezoelectric ceramic plate in capacitance and battery. When the external excitation is close to the natural frequency of the piezoelectric generator, the output power of the piezoelectric transducer can reach the maximum value of 2 mW. In 2002, Ottman and co-workers<sup>[25]</sup> improved the piezoelectric energy storage circuit, making the piezoelectric transducer components to achieve the best value and store in a chemical battery. The piezoelectric energy storage circuit includes a dc–dc buck converter, synchronous waveform corrector, capacitors and chemical batteries. In the energy storage circuit, using the timing control circuit and changing the switching frequency of the dc–dc buck converter can ensure that the flow into the battery achieve the best and improve the charging current. It was found that when the piezoelectric energy storage circuit charged the battery, the amount of electricity stored in the battery was four times that of the original circuit. This group also<sup>[26]</sup> improved the power of the piezoelectric energy harvesting device energy output. The circuit

used in that research had high energy consumption in the pulse control part. Therefore, they initially put the control part of the circuit and use a pulse charging circuit to produce a continuous duty factor and get test results.

In 2016, Azizi et al.<sup>[27]</sup> investigated the mechanical behavior of a bimorph piezoelectric micro cantilever exposed to harmonic base excitation and concluded that the energy harvesting in the absence of mechanical damping resembles the behavior of a damped mechanical oscillator due to the exponential attenuation of the motion amplitude. Their test showed that the output power in terms of the load resistance of the output circuit exhibits Lorentzian behavior, revealing the multifactorial dependency of the power on the governing parameters, and illustrated that the amplitude descends exponentially resembling the behavior of a damped single degree of freedom oscillator; the equivalent nondimensional damping coefficient was determined so that the temporal response fits with an equivalent damped oscillator based on the least square error.

In 2017, Pillatsch et al.<sup>[28]</sup> investigated the possibility that microcrack formation in the piezo layers under tension would be a key mechanism of degradation. They performed tests on bi-layer harvesters that maintain the two layers entirely in tension or compression, demonstrated degradation to happen primarily within the tensile layer, and supported the proposition that microcracking was responsible. This indicates that a possible solution can be to fabricate harvesters where the piezo layers are prestressed in compression. In recent years, different reviews over piezoelectric energy harvesters have been carried out, each focusing on a specific aspect of piezoelectric harvesters in terms of materials, designs, and applications. In recent years, different reviews over piezoelectric energy harvesters have been carried out, each focusing on a specific aspect of piezoelectric harvesters in terms of materials, designs, and applications (summarized in **Table 2**).

The piezoelectric effect can be divided into two areas: the direct effect and the converse effect. The direct effect describes a piezoelectric material's properties to convert mechanical strain and pressure into electrical energy. The converse effect is the opposite, which is the conversion of electrical energy into a mechanical force. These effects are shown in **Figure 2A** and are described by the following equations<sup>[37,38]</sup>

Direct piezoelectric effect

$$D_i = e_{ij}^\sigma + d_{im}^d \sigma_m \quad (1)$$

Converse piezoelectric effect

$$\varepsilon_k = d_{jk}^c E_j + S_{km}^E \sigma_m \quad (2)$$

Vector  $D_i$  is the dielectric displacement in  $\text{N m}^{-2}$ ,  $\varepsilon_k$  is the strain vector,  $E_j$  is the applied electric field in  $\text{V m}^{-1}$ , and  $\sigma_m$  is the stress vector in  $\text{N m}^{-2}$ . The piezoelectric constants are the piezoelectric coefficients  $d_{im}^d$  and  $d_{jk}^c$  in  $\text{m V}^{-1}$ , the dielectric permittivity  $e_{ij}^\sigma$  in  $\text{N V}^{-2}$ , and  $S_{km}^E$  is the elastic compliance matrix in  $\text{m}^2 \text{N}^{-1}$ . The subscripts c and d refer to the converse and direct piezoelectric effect and the superscripts  $\sigma$  and  $E$  show that the quantity measured is at constant stress or electric field.

A material is considered a piezoelectric material when it can transform mechanical strain into electrical energy via the

**Table 2.** Summary of recent studies on MEMS-based piezoelectric energy harvesters.

Reference	Year	Research focus	Key contributions
McCarthy et al. <sup>[16]</sup>	2016	Novel application	– The importance of fatigue damage due to cyclic stresses, efficient space and aerodynamic design, and ambient circumstances is highlighted
Khan et al. <sup>[29]</sup>	2016	Advanced material manufacturing and new application in thin films	– The progress in manufacturing and quality of the thin-film surface is depicted. – The optimization of deposition conditions in thin-film substrates is carried out.
Priya et al. <sup>[30]</sup>	2017	Material structure quality enhancement	– Introduced the higher power density and wider bandwidth of resonance as the two biggest challenges than the compactness, output voltage, operating frequency, input vibration amplitude, lifetime, and cost. – Listed the recent studies analyzing power densities of piezoelectric energy harvesters.
Narita and Fox <sup>[31]</sup>	2017	Novel piezoelectric material fabrication	– The limitation of piezoelectric harvesters due to high impedance, which reduces the charge productions is focused. – The need for accurate multiscale computational methods and piezoelectric in terms of science of material, e.g., fracture and fatigue studies and durability is highlighted.
Abdelkefi <sup>[32]</sup>	2016	Mathematical modeling and design	– Explained the nonlinear effects of the piezoelectric materials, considering aerodynamic force – Analyzing the piezoelectric sheets and characteristics of the layers.
Yildirim et al. <sup>[33]</sup>	2017	Hybrid method design	– The importance in development of amplification techniques, resonance tuning methods and introducing nonlinear oscillations are mentioned.
Wei and Jing <sup>[71]</sup>	2017	Mathematical modeling and novel implementation	– The significance of materials, the change in the stress direction, alteration of the electro pattern is depicted – The challenges in depolarization, brittles in bulk piezolayer and poor coupling in piezo-films are highlighted.
Briscoe and Dunn <sup>[4]</sup>	2015	Material coupling advancement	– The approach of enhancing the coupling of piezodevices is showed.
Ali et al. <sup>[15]</sup>	2019	Novel application	– The flexibility and durability of piezoelectric generators for adopting to human body are highlighted. – The importance of power management, medium for electric connection, biological safety in biomedical application are directed.
Yan et al. <sup>[34]</sup>	2019	Design Mechanism	– Presented a good literature summary for design and structure formation of energy harvesters. – The superiority of impact-based techniques are highlighted and compared with the bending techniques.
Elahi et al. <sup>[35]</sup>	2018	Mechanism Application Assessment method	– The need for improving aerodynamic models in steady, quasi-steady, or unsteady aerodynamics are mentioned. – The significance of attached battery terminals design are depicted. – The importance of material development with higher coupling coefficient are highlighted. – Suggested for the development of under-water and within-electronic-devices applications.
Sezer et al. <sup>[36]</sup>		Principle, structure, operational modes, materials, and applications	– A comprehensive review on piezoelectric energy harvesting systems – Wide range of applications are summarized

direct piezoelectric effect and transform electrical energy into a mechanical movement using the inverse piezoelectric effect. Any stressing or deformation on the body of material will generate an electric current that can be harvested at any point on the material. A voltage of the same polarity as the polarizing electric field will be created if the material is compressed and a voltage of the opposite polarity will be generated if the material is stretched.<sup>[42]</sup>

All ferroelectric materials, which are materials with an electric polarization that can be spontaneously reversed through the use of an electric field,<sup>[43]</sup> are piezoelectric materials.<sup>[43]</sup> The molecular structure of a ferroelectric material is arranged in a way that exhibits an electric dipole;<sup>[42]</sup> however, an applied electric field can cause the dipoles to reorient themselves in the direction of the electric field, which is a process called poling. The dipoles remain in this orientation after removing the electric field, and a poled ferroelectric material will exhibit the

piezoelectric effect.<sup>[39]</sup> To describe the polarity, a sign convention is used for piezoelectric materials. The sign convention here will be generalized to two modes: the  $d_{33}$  mode and the  $d_{31}$  mode. The subscripts 3 and 1 refer to directions in the piezoelectric material which is shown in Figure 2B.<sup>[39,40]</sup>

The  $d_{33}$  mode indicates that the direction of the electric field is parallel to the direction of mechanical strain, and the  $d_{31}$  mode is used when the directions of the electric field and mechanical strain are perpendiculars. MEMS devices have typically used a piezoelectric arrangement which involves a piezoelectric material held between two electrode layers. The voltage ( $V_{31}$ ) generated by the  $d_{31}$  layout is proportional to the stress applied ( $\sigma$ ), the thickness of the piezoelectric material ( $t$ ), and the piezoelectric voltage constant ( $g_{31}$ ).<sup>[40]</sup> The equation is shown as follows

$$V_{31} = \sigma \times g_{31} \times t \quad (3)$$

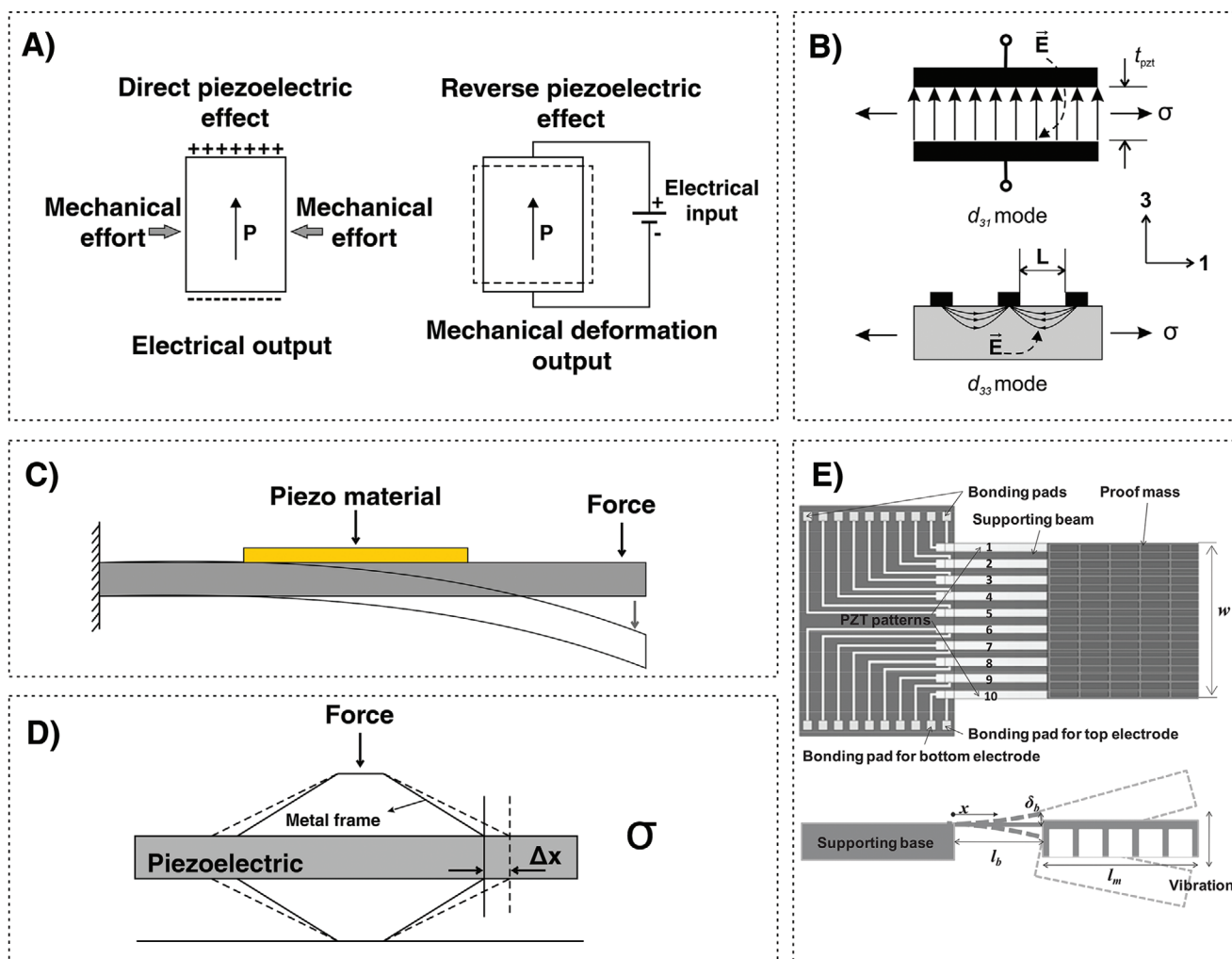


**Figure 2.** Fundamentals and structures of piezoelectric energy harvesters. A) Diagram of the direct and converse piezoelectric effects. B) The directions for the piezoelectric naming conventions. The  $d_{31}$  (left) and  $d_{33}$  (right) methods of energy harvesting. Adapted with permission.<sup>[40]</sup> Copyright 2012, Cambridge University Press. C) A cantilever type piezoelectric energy harvester. Vibrations causes the mass on the end to wobble which generates a current in the piezoelectric material in the beam. D) A cymbal type piezoelectric energy harvester with the piezoelectric material surrounded by two metal sheets. E) Schematic illustration of piezoelectric cantilever in top view and side view. Adapted with permission.<sup>[40]</sup> Copyright 2012, Cambridge University Press.

The effectiveness of  $d_{31}$  piezoelectric for energy harvesting purposes is reduced due to the low thickness of the piezoelectric material, which is typically below  $1 \mu\text{m}$ . This low thickness reduces the voltage that can be gained from the piezoelectric effect, limiting the ability of a  $d_{31}$  piezoelectric material to harvest energy.<sup>[40]</sup> The  $d_{33}$  piezoelectric materials are sometimes able to produce more voltage. However, considering the advances in  $d_{31}$  piezoelectric materials, both layouts are viable for energy harvesting. The two modes of piezoelectric harvesting are shown in Figure 2C.<sup>[40]</sup>

### 2.1.1. Recent Design Considerations

A piezoelectric generator is a device that uses the piezoelectric effect to create an electrical current. The piezoelectric effect is a property of certain crystalline materials such as quartz and these materials can be broken into several categories including

piezoceramics and piezopolymers. The advantages of using piezoelectric materials over other forms of energy harvesters such as electrostatic and electromagnetic have been theoretically shown by the author of ref. [44], who claims that the energy density of piezoelectrics is around four times higher than electrostatic and electromagnetic devices. Piezoceramics are a ubiquitous piezoelectric material used for energy harvesting purposes. There are many different methods of using piezoceramics materials for energy harvesting. The most common structures using piezoceramics are the cantilever type and cymbal type described in the following.

A piezoelectric cantilever consists of a beam element supported on one end and is free to move on the other. The beam typically consists of a piezoceramics material that is attached to an elastic material. A load or mass on the beam's free end causes the beam to vibrate, generating electricity in the piezoelectric material. A diagram of a cantilever piezoelectric device is shown in Figure 2D. The manufacturing of a MEMS



piezoelectric cantilever type energy harvesting is described in ref. [42].

Roundy et al.<sup>[9]</sup> examined the difference in potential power density between a capacitive MEMS and a cantilever type piezoelectric converter and experimented with the accuracy of their calculations using a commercially available PZT piezoelectric bimorph. The authors showed that powering a small wireless device using ambient vibrations is feasible for certain applications through the use of piezoelectric materials. They also demonstrated that piezoelectric converters are capable of converting more power per cubic centimeter than capacitive converters. The authors were able to achieve a power density of  $70 \mu\text{W cm}^{-3}$  using the PZT bimorph; however, they deduced it was theoretically feasible to achieve a power density of  $250 \mu\text{W cm}^{-3}$ .

Roundy et al.<sup>[45]</sup> have also investigated piezoelectric materials, where the design of a two-layer cantilever piezoelectric generator was designed and optimized. The authors provide an in-depth analysis of the mechanics and theory behind the composite piezoelectric beam, then analyze which is beyond this paper's scope. The authors construct the beam using two layers of PZT-5A sandwiching a steel center shim with a large mass resting on the beam's free end. This design differs from previous designs, which only had two layers; one layer of a piezoelectric material and one suitable flexible material. The authors found that their piezoelectric harvester yielded a power output of  $375 \mu\text{W cm}^{-3}$  from a 120 Hz vibration source at  $2.5 \text{ m s}^{-2}$ .

Among common piezoelectric structures in MEMS, i.e., cantilever, doubly supported beam, diaphragm, the cantilever can be better for a given input force. Thus, the normal state of the piezoelectric generator is a composite microcantilever with an optional metal mass. The microcantilever tends to have a relatively high natural frequency, so the metal mass on the tip (free end) of the cantilever is used to decrease the structure's natural frequency to fit the low-frequency vibration work conditions. A piezoelectric thick film is the core of this composite cantilever, which is sandwiched between a pair of metal, usually Pt/Ti electrodes, deployed on an elastic base.

When the base frame of the device is vibrated by the environmental groundwork, at the same time, it inputs a particular force into a secondary mechanical system. This enables the tip of the cantilever to vibrate, and the relative displacement of the cantilever tip and base causes deformation of the piezoelectric material in the system, thereby generating alternating current between the metal electrodes pair. The magnitude of this electric charge voltage is proportional to the stress induced by the relative displacement.<sup>[46]</sup>

A cymbal type piezoelectric device typically consists of piezoelectric material between two metal sheets in a cymbal-like structure with a vacuum between the piezoelectric and metal. A picture of a cymbal-type piezoelectric is shown in Figure 2E. As claimed by the authors,<sup>[41,47]</sup> a cymbal-type piezoelectric device is more robust and resilient compared to a cantilever type and is suitable in areas where the mechanical vibrations are exceedingly large. The authors in ref. [48] also note the enhanced endurance of cymbal piezoelectrics due to the high strength steel cap and claim that cymbal-type piezoelectrics are suitable for forces around 100 N at frequencies 100–200 Hz.

The authors in ref. [48] tested their cymbal transducer at a force of 70 N and a frequency of 100 Hz. They found that the

device was able to generate 52 mW of power across a 400 k $\Omega$  resistor. The authors also showed that a PZT material with 1 mm thickness yielded the highest power output. In ref. [49], the authors used a device made up of two ring-type piezoelectric stacks, one pair of bow-shaped elastic plates, and one shaft that precompresses them. They found that in this configuration, the piezoelectric device without an electric load could generate a maximum electric peak-to-peak voltage of 110 V, and with a load of 40 k $\Omega$ , the maximum power output was 14.6 mW at a frequency of 87 Hz.

Also, a stack type piezoelectric device is able to produce a large amount of energy due to several layers of piezoelectric materials stacked together.<sup>[38]</sup> The authors explored the efficiency of a stack type piezoelectric device in ref. [50] and examined the dielectric and piezoelectric properties of the device. The authors found that under an external force at 120 Hz, the piezoelectric stack produced a voltage of 12 V and a power of 60 mW. Also, the authors in ref. [51], used a stack configuration to harvest broadband vibrational energy. The piezoelectric stack was analyzed with and without electric inductance, and the authors showed that to maximize the harvested power, the mechanical damping in the device should be minimized while the electromechanical coupling should be maximized.

In ref. [52], the authors compared four vibration-powered energy harvesters, designed to power standalone systems. They proposed a synchronized switch damping (SSD) system to be used for energy scavenging and claimed that SSD was able to increase the amount of converted energy resulting from the piezoelectric material.

Piezopolymers are advantageous over their ceramic counterparts as they are ductile, lightweight, resilient to shock, and deformable.<sup>[38]</sup> The authors in ref. [53] investigated the energy harvesting capabilities of an electrostrictive terpolymer composite filled with 1 vol.% of carbon black polyvinylidene fluoride-trifluoroethylene-chlorotrifluoroethylene. The authors note that piezopolymers are suitable for devices, which require high flexibility, such as textiles. They are also easier to implement since they do not require thermal treatment and can be obtained in a variety of shapes and sizes. The authors compared the carbon-filled terpolymer with other piezopolymers and found that it outperformed them by a significant margin, and was 2000 times more effective than pure polyurethane.<sup>[53]</sup>

The authors in ref. [54] compared the energy scavenging capabilities of a piezoelectric PZT ceramic, polyvinylidene fluoride (PVDF) membrane and polypropylene (PP) foam polymer in an attempt to generate power from ambient vibrations. The authors directly compared how different ceramic fiber diameter, laminate thickness, impact area, the weight of the free-falling mass, vibration frequency, and temperature would affect the voltage output.

In ref. [17], the authors designed and analyzed an energy harvester named piezoelastica energy harvester (PEEH) to harvest ambient mechanical energy present in flex cable kinetic and vibratory motions. The device was primarily used to harvest energy from a computer hard disk drive. The authors observed that their proposed device could harvest around 25% of the power used by the hard disk drive. This scavenged energy primarily came from the device's swinging rotary actuator between the disk's outer and inner regions, while around a third of the

scavenged energy came from the bending of the device. This highlights the possibility of using energy harvesting piezoelectric devices to increase the electronic efficiency of simple machines.

### 2.1.2. Recent Fabrication Strategies

Since the frequency of the surrounding vibration sources is relatively low (less than 200 Hz) compared to the natural frequency of the materials to make up the microgenerator, the fabrication of such devices with a low resonant frequency while reducing the size microscale is quite challenging. In this part, several fabricating methods will be stated.

A study presented by Huicong Liu<sup>[41]</sup> about piezoelectric energy harvesting explains the design, microfabrication and measurement of this device, used for harvesting energy from environmental vibrations of low frequency. This study concentrates on thin-film patterns (PZT patterns), where they are arranged in parallel with a supporting cantilever, as shown in Figure 2E, which illustrates the piezoelectric cantilever from the top view.

3D printing is used to fabricate piezoelectric materials in different systems.<sup>[55,56]</sup> The development of the 3D printable piezoelectric materials has led to the fabrication of integrable sensors in a single-step printing process without poling, which is important to creating a wide variety of smart structures. A method is the addition of barium titanate nanoparticles in nucleating piezoelectric  $\beta$ -polymorph in 3D printable polyvinylidene fluoride (PVDF) and fabrication of the layer-by-layer and self-supporting piezoelectric structures on a micro- to millimeter-scale by solvent evaporation-assisted 3D printing.<sup>[57]</sup>

The microstructures of piezoelectric energy harvesters have been fabricated using digital projection printing. By Kim et al.,<sup>[58]</sup> piezoelectric polymers have been fabricated by incorporating barium titanate (BaTiO<sub>3</sub>, BTO) nanoparticles into photolabile polymer solutions and exposing to digital optical masks which can be dynamically altered to generate user-defined 3D microstructures. Also, the 3D printing process in the fabrication of ceramic piezoelectric components has been investigated using a high solids loading slurry with the nanoparticle, by Chen et al.<sup>[59]</sup>

Tomasz Zawada,<sup>[60]</sup> illustrated how vibrations could be used as an energy source, ultimately converting them into a usable electrical signal. Unlike the process mentioned by,<sup>[41]</sup> he explains a silicon cantilever with complete PZT thick film and uses the screen-printing method simultaneously. Experiments were conducted on thick film materials with pressure treatment and compared with standard thick films. Finally, the author found that the structures based on the pressure treated materials had perfect properties as for the energy output.

As for the fabrication process, double-side polished SOI wafers (450  $\mu\text{m}$ ) have been used by Marzencki et al.,<sup>[61]</sup> where the buried oxide layer (150 nm) is used as a stop layer for deep reactive ion etching from both sides. The details for structure and application are described in ref. [61].

In regard to piezoelectric microcantilever fabrication, Fang et al.<sup>[45]</sup> used microfabrication techniques, mainly involving functional films pattern, bulk silicon micromachining, structure

release, and mass assemblage. Recent progress of piezoelectric energy harvesting technologies based on PZT materials is gathered in ref. [62]. These fabrication types are based on flexible piezoelectric energy harvesting devices using the PZT and flexible materials, including nanotubes,<sup>[63]</sup> nanorods,<sup>[64]</sup> nanowires,<sup>[65]</sup> nanofibers,<sup>[66]</sup> nanocomposites,<sup>[67]</sup> besides thin films.

### 2.1.3. Practical Applications and Output Performance

Each application has its own vibration peaks, so a device with a single resonance frequency can only be used in a specific application. To tackle this problem, Marzencki et al.<sup>[61]</sup> proposed a way to tune the resonance frequency of energy harvester device. This simple method uses the mechanical nonlinear behavior of structures under large deflections. Two kinds of piezoelectric vibration energy harvesters have been provided, one is called clamped-free MEMS energy harvester and the other is called clamped-clamped MEMS energy harvester.

A new type of electronic cigarette lighter<sup>[68]</sup> is made of piezoelectric ceramics. As long as the finger press the lighter button, the lighter on the piezoelectric ceramic can produce high pressure to form electric spark and ignite the gas, which can be used for a long time.

Also, MEMS-based piezoelectric harvesters are applied to accelerometers. Generally, an accelerometer behaves as a damped mass on a spring. When the accelerometer experiences an acceleration, the mass is displaced to the point that the spring can accelerate the mass at the same rate as the device's housing. Thus, piezoelectrics, besides piezo resistive and capacitive components, are commonly used to convert mechanical motion into an electrical signal in commercial devices. Piezoelectric accelerometers<sup>[69]</sup> rely on piezo ceramics or single crystals and are preferred for applications requiring operations in upper frequencies and temperature ranges and having low package weight.

In the case of a strong shock, using piezoelectric materials, the microprocessor triggers the safety devices suited to a particular situation, e.g., electromagnetic door-openers, safety belts with pyrotechnic tightening action, inflatable air bags, and loosening devices for safety belts. Various mechanisms have been proposed for this purpose.<sup>[70,71]</sup> A piezoelectric blade protection structure is presented for a plurality of juxtaposed piezoelectric blades mounting onto a circuit board to provide protection and anchoring effect for the piezoelectric blades.<sup>[72]</sup>

Piezoelectric energy collection has been applied to highway pavement to harvest the vehicle road vibration and generate power to supply electric energy for road lamps and other road infrastructure or be put into the storage device for further use. As described by Xu et al.<sup>[73]</sup> the system comprises a piezoelectric power generation device, a power conversion device, and a road lamp or an energy storage device arranged on the road surface. This can effectively solve the problems of inconvenient installation of lamps and lanterns in mountainous areas and long-distance roads to meet the requirements of energy-saving and environmental protection.

The development in microscale piezoelectric energy harvesters has produced simple and highly efficient self-powered sensor systems by harvesting the mechanical energy from the

ambient environment. According to ref. [5], a self-powered microfluidic sensor harvesting the mechanical energy of the fluid and simultaneously monitoring their characteristics has been fabricated by integrating the flexible piezoelectric polyvinylidene fluoride (PVDF) nanofibers with the well-designed microfluidic chips. Those devices could generate open-circuit high output voltage up to 1.8 V when a droplet of water was flowing past the suspended PVDF nanofibers, which resulted in their periodical deformations. The impulsive output voltage signal allowed them to be utilized for droplets or bubbles counting in the microfluidic systems.<sup>[5]</sup>

Also, in another case, a microfluidic structure is designed, whose damping motion is used for energy harvesting. This microfluidic chip is based on a microfabricated electret silicon oxide (SiO<sub>2</sub>). When the device was subjected to an instantaneous acceleration, the power was generated due to the variable shape of the microfluidic on the electret film. The damped wave phenomena came from the variable shape of microfluidic, which oscillated back and forth due to inertial forces.<sup>[74]</sup>

## 2.2. Electromagnetic Energy Harvesting

Energy harvesting through electromagnetic MEMS devices (electromagnetic generators or (EMS)) is a well-established field due to the simplicity of their design and thoroughly understood the theory of electromagnetic induction.<sup>[75]</sup>

First discovered in 1831 by Michael Faraday, electromagnetic induction produces an electromotive force (EMF), which results in a current when a conductor is passed through a varying magnetic field. This is most commonly achieved by using a metal coil as a conductor, moving relative to a magnet. The amount of voltage produced by this form of generator depends on the number of turns in the coil, the strength of the magnetic field and the velocity of the relative motion. Since they rely on external vibrations and require no power input, electromagnetic energy harvesting devices are extremely convenient for supplying low power industrial sensors and vehicle sensors, where they can take advantage of the natural vibrations and maintain a stable output of electricity. They can also serve as an effective replacement for batteries in remote microsensor systems.

Various studies have been conducted, reviewing electromagnetic energy harvesters, and focusing on specific aspects of these harvesters in mathematical modelling, materials, designs, and applications. A part of the recent research in this field is summarized in **Table 3**.

The operational principle of a conventional micromagnetic induction energy harvester is based on Faraday's law; the induced electromotive force in any closed circuit is equal to the rate of change of the magnetic flux in time.<sup>[76]</sup> It can be described as follows

$$|\varepsilon| = \left| \frac{d\varnothing_B}{dt} \right| \quad (4)$$

where  $\varepsilon$  is the magnitude of electromotive force,  $\varnothing_B$  is the magnetic flux (in a magnetic field) through a circuit. This formula shows that the change in the magnetic flux through a circuit induces an electric current. The conventional structure of a

micromagnetic induction energy harvester system involves a rotor producing changing magnetic flux called as moving element and an associated coil termed stator.<sup>[83]</sup>

### 2.2.1. Recent Design Considerations

Williams and Yates did the earliest analysis of electromagnetic induction-based energy harvesting MEMS in 1995; this publication outlined the design of a device modelled as a spring–mass–damper system where the magnet is the mass; a cantilevered beam is used as a spring, and the transducer behaves as a damper. They confirmed that the maximum power output is achieved at frequencies about the resonant frequency of the spring–mass–damper system. They also theoretically showed that the power output of a device is proportional to the cube of the frequency.<sup>[84]</sup>

Neil et al. developed a laser-micromachined multimodal resonating power transducer capable of powering commercial IR remote control systems. A laser micromachined spiral copper spring was used to convert the vertical vibration of the device to the horizontal vibration of the internal magnet, which gave significantly higher output voltage. The final device had a volume of fewer than 1 cm<sup>3</sup> and provided a power between 200 and 830  $\mu$ W for frequencies of 60–110 Hz and vibration amplitude of 200  $\mu$ m.<sup>[85]</sup>

In 2006 Saha et al. explored the optimized conditions of a typical electromagnetic microgenerator. They compared the theoretically derived conditions against experimental data obtained from two different prototyped microgenerators. They were able to show that the maximum power output is achieved when the electromagnetic damping is equal to the parasitic damping in the system. The parasitic damping is the damping due to air resistance and material loss. In their experiments, they were able to show that despite reasonable differences between the expected and experimental results, the optimization conditions were consistent.<sup>[86]</sup>

An electromagnetic microgenerator optimized for low ambient vibration was developed by Beeby et al. in 2007. For an overall size of less than 1.5 cm<sup>3</sup> the generator uses four magnets in pairs on an etched cantilever with a coil residing between two of the pairs of magnets. The microgenerator produced 46  $\mu$ W at a frequency of 52 Hz; this frequency was designed so that the microgenerator would be optimized for placement on an air compressor unit with resonances between 43 and 109 Hz overall indicative of the conditions found in many industrial applications. The microgenerator was estimated to deliver 30% of the power supplied from the environment to usable electrical power.<sup>[87]</sup> In the same year, a low-cost electromagnetic microgenerator capable of being fabricated in batches was developed by Wang et al. This prototype is manufactured using traditional MEMS manufacturing techniques including etching, sputtering and electroplating to create the copper spring that houses a permanent magnet and the copper coil that cuts the magnetic field. The device could produce a peak-to-peak voltage of 60 mV with an amplitude of vibration of 738  $\mu$ m at a resonance frequency of 121.25 Hz. The prototype also showed good agreement to the results of an ANSYS simulation, validating the simulation to test further designs.<sup>[88]</sup>



**Table 3.** Summary of recent studies on MEMS-based electromagnetic energy harvesters.

Reference	Year	Research focus	Key contributions
Tan et al. <sup>[76]</sup>	2016	Novel application and performance check	<ul style="list-style-type: none"> <li>– Categorized the electromagnetic harvesters in reducing the resonant frequency, broadening the frequency band of vibration, and improving the compatibility with the MEMS system.</li> <li>– The necessity to use batteries along with energy harvesters rather than replacing batteries are depicted.</li> <li>– The need for the development of design and manufacture of the spring, planar inductive coil, simulation accuracy, and magnet electroplating technology in electromagnetic energy harvesters are highlighted.</li> </ul>
Yildirim et al. <sup>[33]</sup>	2017	Hybrid method Design	<ul style="list-style-type: none"> <li>– Presented the hybrid techniques for performance enhancement in energy harvesters.</li> </ul>
Wei and Jing <sup>[11]</sup>	2017	New application and mathematical modeling	<ul style="list-style-type: none"> <li>– Referred to low cost and easy fabrication process of electromagnetic energy harvesters, compared to piezoelectric and electrostatic harvesters.</li> <li>– The limitations in coil spaces, while existing a need to reduce space are mentioned.</li> </ul>
Zergoune et al. <sup>[77]</sup>	2019	Performance check and new design	<ul style="list-style-type: none"> <li>– Proposed methods for enhancing effective bandwidth and harvesting power.</li> </ul>
Abdelkareem et al. <sup>[77]</sup>	2018	New application for harvesting vehicle suspensions	<ul style="list-style-type: none"> <li>– The need to improve the techniques for using energy dissipated in traditional hydraulic shock absorbers as an energy source for electromagnetic energy harvesters is depicted.</li> <li>– Presented different electromagnetic harvesting-based dampers.</li> <li>– Introduced the potential concerns, such as the compactness and nonlinearity of the harvesters.</li> </ul>
Naifar et al. <sup>[78]</sup>	2017	Performance check and new design	<ul style="list-style-type: none"> <li>– Compared the recent electromagnetic devices in terms of delivered energy, type of vibration excitation, energy outcome, and working frequency.</li> <li>– Highlighted the challenges of electromagnetic energy harvesters in miniaturized devices.</li> </ul>
Le et al. <sup>[79]</sup>	2015	Novel application in health monitoring sensors	Described electromagnetic energy harvesters more effectively in the low-frequency range (<100 Hz) than piezoelectric one.
Siddique et al. <sup>[80]</sup>	2015	Hybrid technique-based design and implementation	<ul style="list-style-type: none"> <li>– Referred to narrow operating bandwidth and inconsistency in environmental vibrations as the challenges. The need to develop new cantilever designs, improve strain by maximizing the proof mass, develop tuning circuit to achieve the resonant frequency, enlarge effective bandwidth, implement frequency up conversion technique, and apply nonlinear dynamical systems are highlighted.</li> </ul>
Wang et al. <sup>[81]</sup>	2018	Novel application	<ul style="list-style-type: none"> <li>– Depicted the easy installation process and a great success rate of electromagnetic energy harvesters in structural health monitoring of bridges.</li> <li>– Showed the unsuitability of electromagnetic harvesters for adopting directly to pavement vibrations.</li> </ul>
Choi et al. <sup>[82]</sup>	2019	Implementation for sound energy harvesting	<ul style="list-style-type: none"> <li>– Listed recent researches in sound energy harvesting techniques.</li> <li>– Categorized sound energy harvesters as pressure amplification method and transduction mechanism.</li> <li>– Found electromagnetic sound energy harvesters as those with lower load impedance than piezoelectric and triboelectric types.</li> </ul>

In 2010, Zhu et al.<sup>[89]</sup> developed an electromagnetic micro-generator with a tunable resonant frequency, enabling the generator to be adjusted to maximize its power output to suit the particular application. The system is tuned by varying the distance between two tuning magnets from 5 to 1.2 mm, corresponding to resonant frequencies of 676 to 98 Hz. The device had a volume of  $\approx 2 \text{ cm}^3$  and a power output of 61.6 to 156.6  $\mu\text{W}$  over its tuning range with a vibration acceleration level of  $0.59 \text{ ms}^{-2}$ .

Turkylmaz et al.<sup>[90]</sup> designed a potential second-generation electromagnetic MEMS power generator intended for harvesting energy from low-frequency external vibrations. The device used electromagnetic induction with a magnet on the low-frequency actuation plane and coils on the high-frequency resonance plane. A macroscale prototype was developed, which produced maximum power of 5.1  $\mu\text{W}$ . The simulated system provides more than three orders of magnitude improvement in energy efficiency for the ambient vibration range of 70–150 Hz,

compared with first-generation MEMS energy harvesting devices.

In 2012 Rahimi et al.<sup>[91]</sup> designed and developed a fully integrated energy harvesting system capable of converting ambient 8 Hz vibration to a power output of 54  $\mu\text{W}$  through a dual rail 1.46 V DC voltage with a reported system efficiency of 81%. The system involved a double-coil electromagnetic transducer connected to a voltage regulator designed to rectify the input AC voltage with peak amplitude ranging from several hundred millivolts to several volts. The rectifier was powered by a passive network built from low threshold-voltage chip diodes and capacitors. The overall system had a volume of  $16 \text{ cm}^3$  and a power density of  $6.06 \mu\text{W cm}^{-3}$ , three times any previously reported density for a battery-less vibration driven system.

Also, in some cases using piezoelectric materials, researchers have produced hybrid MEMS-based electromagnetic energy harvesters.<sup>[92,93]</sup> In 2016, Xu et al.<sup>[92]</sup> prototyped a novel tunable multifrequency hybrid energy harvester, which consisted of a

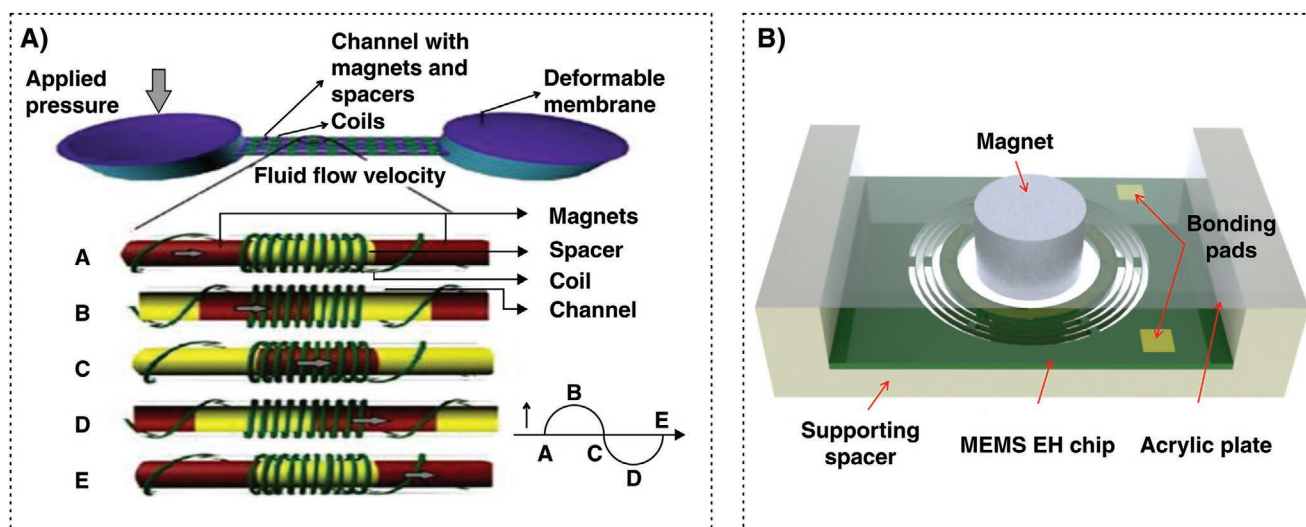


**Figure 3.** A) The structure of a microfluidic-based electromagnetic energy harvesting device. Reproduced with permission.<sup>[96]</sup> Copyright 2015, IOP Publishing. B) The multifrequency MEMS electromagnetic energy harvester device. Reproduced with permission.<sup>[96]</sup> Copyright 2015, IOP Publishing.

piezoelectric energy harvester and an electromagnetic energy harvester, coupled with magnetic interaction. In their design, the measured first peak power increased by 16.7% and 833.3% compared with the multifrequency electromagnetic energy harvester and the multifrequency piezoelectric energy harvester. It was 2.36 times more than the combined output power of the linear piezoelectric energy harvester and linear electromagnetic energy harvester at 22.6 Hz.

In 2018, Radhakrishna et al.<sup>[94]</sup> presented and prototyped the first fully functional integrated low-power interface IC for a MEMS-based electromagnetic vibration energy harvester. The IC accomplished cold startup from a 50 Hz-150-mV-peak AC input to a 1.1 V output. The cold startup was achieved using an on-chip Meissner oscillator with an off-chip transformer. Also, a self-timed current-feedback-based H-bridge circuit was turned on for conjugate impedance matching with on-chip control and an off-chip microcontroller for impedance synthesis. The regular-operation H-bridge circuit delivered 820  $\mu\text{W}$  to a load capacitor at 71% efficiency at resonance.

Recently, two-degree-of-freedom MEMS electromagnetic vibration energy harvesters have been proposed and prototyped by Tao et al.<sup>[95]</sup> They presented a dual-mass resonant structure consisting of a primary mass, while an accessory mass is structured on an SOI wafer by double-sided deep reactive-ion etching (DRIE). In their design, by adjusting the weight of the accessory mass, the first two resonances of the primary mass were tuned close to each other while maintaining comparable magnitudes. Therefore, both resonances could contribute to energy harvesting, which resulted in more efficiency.

### 2.2.2. Recent Fabrication Strategies

The microfluidic electromagnetic energy harvesting device mainly consists of two reciprocal diaphragms, which can be placed respectively at the heel and toes where maximum pressure is alternately exerted from the human walk. This

alternating pressure onto two diaphragms moves magnets between the chambers under diaphragms, producing electromagnetic energy in association with coils around the channels.<sup>[96]</sup> **Figure 3a** shows the structure of a microfluidic-based electromagnetic energy harvesting device.

Huicong Liu et al.<sup>[97]</sup> has developed a multifrequency vibration-based MEMS electromagnetic energy harvester, using a fixed magnet and moving coils flexible and easy to assemble. A circular mass and three circular rings were used to retain the circular suspension structure incorporated with metal coils, and a bulk magnet was fixed above it. The gap distance between the moving coils and the fixed magnet was adjustable. Also, the resonant frequency could be adjusted by the width, thickness and diameters. **Figure 3b** shows the MEMS chip assembled on a supporting spacer. A cylindrical magnet is attached on an acrylic plate in this design and placed at the center of the circular suspension structure.

In order to harvest energy from mechanical vibrations, or otherwise “wasted” mechanical movements, an apparatus is presented, combining magnetic and microfluidic elements to create electrical energy,<sup>[98]</sup> in which authors presented an energy harvesting system for converting mechanical energy into electrical energy based on the interaction between conductive microfluidic droplets and dielectric-coated electrodes in combination with an electromagnetic arrangement based on the interaction between magnetic elements and coils, with the two arrangements disposed of in an interleaved configuration that provides a degree of synergy to the overall system in the form of providing spacings between adjacent elements and providing a bias voltage source for the electrostatic arrangement from the energy created by the electromagnetic arrangement.

### 2.2.3. Practical Applications and Output Performance

As the rapid development and increasingly mature MEMS technology, electronic products become microminiaturized and integrated. The appearance and development of bluetooth

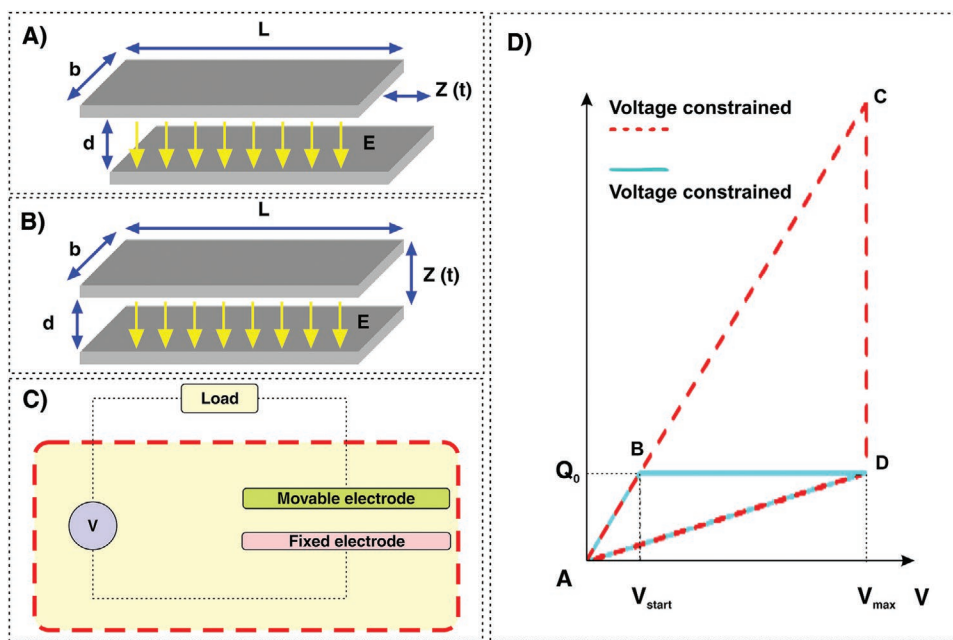


**Figure 4.** Electrostatic vibration energy generators A) in-plane mode and B) out-plane mode. C) A diagram of electrostatic energy harvester system operation. D) Conversion cycles for micro-electrostatic energy harvester.

technology and low power communication standard prompt electronic devices to become wireless and portable. Thus, wireless sensor networks (WSN), embedded system, radio frequency identification (RFID), implantable MEMS sensors and different kinds of new advanced technology make big progress.<sup>[99]</sup> They can be widely applied in video monitoring, building health monitoring, intelligent traffic management, biomedicine, logistics management, and even national defense and military areas. Meanwhile, they can make a huge economic benefit for society.

However, with deep research into wireless sensors and a variety of implantable sensors, how to supply electricity for these devices has become a critical issue to boost its applied research. These devices are usually low power, in  $\mu\text{W}$  order, but often applied in a hard environment, and placed where it is difficult for a human to approach or inside objects' bodies. It has high comprehensive requirements to the volume, cost, working conditions, and power components' life. At present, primary methods to supply electricity such as batteries and corded power are hard to satisfy this requirement owing to short battery life, limited storage energy, relatively largeness compared to sensors, and the fact that disable change on time and corded power cannot satisfy medicine implantable and structure embedded micro sensors' system requirements. Therefore, the research in micro energy harvesting has been an important study field.

### 2.3. Electrostatic Energy Harvesting

The working operation of electrostatic vibration energy harvesters is based on varying capacitance, which makes it possible to use external vibration to change polar plate magnitude from vibrational energy to electrical energy. Two primary modes of motion, in-plane motion and out-plane motion, are depicted in Figure 4A,B.<sup>[100]</sup>

Electrostatic energy harvesters have been of interest to researchers. Table 4 briefly summarizes recent reviewing papers, showing their highlights, applications and main suggestions.

Micro-electrostatic energy harvesting is carried out when the gap of a precharged pair of capacitor electrodes is changed, thereby inducing an electrical field. The process can be seen as mechanical energy, which can move the two electrodes of the precharged capacitor, thereby converting vibrational into electrical energy. In this way, generation in a circuit within the micro-electrostatic energy harvester can be discharged into an external load. The schematic is shown in Figure 4C.

The formula for the capacitance of the capacitor can be presented as<sup>[105]</sup>

$$C(t) = \epsilon A / (g_0 - x(t)) \quad (5)$$

where  $\epsilon$  is the dielectric constant,  $A$  is the plate area,  $g_0$  is the initial gap between the two plates, and  $x(t)$  is the displacement of the movable electrodes. When the movable electrode of the precharged capacitor is moved, the energy of the capacitor electrodes will be changed, followed by an electrical current flow being produced. The external electrical load draws current until the capacitor is discharged. Also, based on the flat plate capacitance formula,  $C = \epsilon Lb$ , regardless of whether top counter electrode moves, horizontally, on the plane, or it moves vertically, against the bottom counter electrode, the capacity between counter electrodes will change.

#### 2.3.1. Recent Design Considerations

Electrostatic vibration energy harvesters have two operation modes, constant charge mode and constant voltage mode,<sup>[106]</sup>

**Table 4.** Summary of recent studies on MEMS-based electrostatic energy harvesters.

Reference	Year	Research focus	Key contributions
Barkas et al. <sup>[101]</sup>	2019	Contribution to reducing greenhouse gas emissions	– The huge scope of potential on both macroscale, e.g., ocean waves, and microscale, e.g., body movements, muscular contractions, blood flow, are highlighted.
Wang et al. <sup>[81]</sup>	2018	Application	– The compatibility and small size of electrostatic harvesters in MEMS processes are outlined. – The promising applications for future wireless sensor networks are unfolded.
Yildirim et al. <sup>[33]</sup>	2017	Hybrid method Design	– Presented the hybrid techniques for performance enhancement in energy harvesters.
Honma et al. <sup>[102]</sup>	2018	Design	– The limitation in the free movement of the suspended electrodes due to electrostatic binding force is described.
Wei and Jing <sup>[11]</sup>	2017	Application Mathematical modeling	– No need for smart materials, and compatibility with small size MEMS applications are illustrated. – The high mechanical damping and sticking probability while operation, high output impedance, low energy density, the need for external voltage are represented.
Choi et al. <sup>[82]</sup>	2019	Triboelectric sound energy harvesters	– Listed the recent researches in sound energy harvesting technology. – Categorized sound energy harvesters as pressure amplification method and transduction mechanism. – The limitations in the performance of triboelectric sound energy harvesters while applying the pressure amplification methods together are highlighted.
Wu et al. <sup>[103]</sup>	2018	Design Application	– The vast range of application in both macro- and microscale are depicted. – The possibility to adopt into the high voltage applications are outlined. – Presented a road map of triboelectric harvesters development from 2017 to 2027.
Kim et al. <sup>[104]</sup>	2019	Design Theory	– Categorized the triboelectric nanogenerators based on both kinematic energy conversion systems and vibrational energy conversion systems. – The importance of optimized mechanical energy conversion systems design to improve the output of triboelectric nanogenerators is highlighted.

as depicted in Figure 4D. For the constant charge mode, the voltage increases as the capacitance decreases; contrarily, for the constant voltage mode, the charge decreases as the capacitance decreases.

These changes can result in an altering of first electrical power. Thus, external vibration makes counter electrodes move and transfer vibrational energy to electrical energy. Because electrostatic reprography transducer has a high order requirement to structure parameter, many components adopt silicon micromachining technique to manufacture electronic comb structure, which is easy to combine with various MEMS.

The changes in capacitance are caused by kinetic inputs, e.g., vibrations, shocks, etc. As shown by Figure 4D, path A–B–D–A represents the constant charge conversion mode and path A–C–D–A displays the constant voltage conversion mode. As most devices are designed to function under a stable current flow, the length of each droplet flowing through the micro-channel must remain constant from one substance to the next. This ensures a constant generation of electricity that enables this type of energy harvester to be used in place of conventional power supplies that commonly run various MEMS devices.

### 2.3.2. Recent Fabrication Strategies

Within the last few years, a new type of energy harvesting technology has presented, which is called a triboelectric nanogenerator (TENG). This is also to harness ambient mechanical vibrations. This technique, reported first in 2012,<sup>[107,108]</sup> utilizes

both electrostatic induction and triboelectric effect,<sup>[109]</sup> and possesses advantages such as high power density, cost efficiency, light weight, small size, flexibility, and transparency.<sup>[110,111]</sup>

The triboelectric effect is a charge transfer method whereby two different materials become electrically charged in opposite signs after contact. Although the origin of this phenomenon is not clearly understood physically, and it is only known that the triboelectric charges are confined on the surface of materials.<sup>[112]</sup> However, the difficulty of applying this technique to be used in power generation was that triboelectric charges were immobile and difficult to be conducted away. Thus, before the arrival of TENGs, it was used to produce high voltage. The key feature of the TENG is to incorporate electrostatic induction into an electricity-generating process, which made mobile charging possible.<sup>[109]</sup> Moreover, the development of hydrogel, the aggregation of crosslinked polymer networks in water,<sup>[113]</sup> with extraordinary electromechanical properties, has solved the challenge of providing high stretch ability and transmittance in TENGs being applied to the new electrodes. Previous efforts have been made to apply hydrogel to contact materials or electrodes of TENGs.<sup>[114]</sup>

Different structures for harvesting a broad range of mechanical energy have been presented, and attractive applications of this technology in energy harvesting are demonstrated. Currently, four basic modes of TENG are presented, including vertical contact-separation (CS) mode, lateral sliding (LS) mode, single-electrode (SE) mode, and freestanding triboelectric-layer (FT) mode.<sup>[111]</sup> Each of these modes has its own specific structure, materials as and mechanical triggering configurations. As



an example, CS mode is triggered by a vertical periodic driving force, causing a repeated CS of two dissimilar materials with coated electrodes on the top and bottom surfaces. As for the LS mode, it is triggered by an LS motion between two dissimilar materials in parallel.<sup>[115]</sup> More recently, by the emergence of artificial intelligence, certain endeavors have been made for the development of AI-TENG or AI-piezoelectric nanogenerators (AI-PENG) to surpass the challenges exist in their fabrication, design, analysis, and application.<sup>[116]</sup>

### 2.3.3. Practical Applications and Output Performance

The leading trend for energy harvesting using microfluidics has been to exploit electrostatic forces, using varying capacitance to generate electricity. Electrostatic fields vary in intensity directly in proportion to the area of the electrode plates. They interact with and inversely in proportion to the square of the distance. This behavior gives two variables that can be altered in order to induce current flow and produce electricity. Using microfluidics, Yıldırım and Kùlah<sup>[117]</sup> have experimented with an alternative way to make use of this phenomenon. They developed a microfluidic device that harvests energy using electrostatic principles. A current can be induced in these types of harvesting devices by varying the capacitance across two electrodes that are separated by an insulating material. This generated electricity can be used to run the device itself or even other devices that are connected to it.

Using some form of mechanical actuation, a series of dielectric droplets can be moved in and out of alignment with strategically placed electrodes, causing current to flow in alternating directions. This method can have limitations due to some effects that govern energy generation. Such limitations include charge trapped in the contact surface where the liquid and solid elements interact as well as the delay introduced by the wetting and dewetting process. However, choosing the correct thin film coating for the contact layer can minimize these effects. These ideas were summarized well in the work of Krupenkin and Taylor.<sup>[118]</sup> They also highlighted three alternate geometric methods for a droplet and electrode configuration that can be used to generate electricity through various forms of mechanical actuation. The first is an out of the plane movement that is actuated by oscillation. As seen in **Figure 5a1**, an array of droplets can be placed spanning the area of two electrodes. By varying the distance between the plates through some form of vibration, the capacitance in the circuit can be changed, causing the current to flow. The second method is seen in **Figure 5a2** is that of a sliding movement that has strips of electrodes that are moved back and forward over the droplets to alter capacitance. The final method, depicted in **Figure 5a3**, uses pressurized droplet flow to actuate the device. The advantage to this method over the other two is the fact that it can be adapted to allow a device to be built without any solid moving parts as it generates electricity purely from fluid flow. All three methods exploit the principle of energy generation through variable capacitance shown in **Figure 5a4**. A schematic of these three methods being used in the application is shown in **Figure 5b**. Triches et al.<sup>[107]</sup> and Meninger

et al.<sup>[119]</sup> designed an energy scavenging technique (**Figure 5c**), combining microfluidics with electrostatic energy harvesting together. The method uses droplet-based microflow of two phases with different electrical permittivities. As a result, a capacitance change across the microchannel to harvesting electrical energy. This technique is implemented on 3 mm wide as well as 1 mm deep mini channels. It is shown that 0.4 nW can be harvested using a single electrode pair, with air or water as the two phases flowing at the speed of 1 mL min<sup>-1</sup>. The generated power can be amplified by microscale implementation. Implementation of this technique in microscale can be a promising way of harvesting energy for low-power systems.

## 3. Thermoelectric Energy Harvesting

In all-natural environments, there is an explicit presence of heat. Biological organisms convert reservoirs of chemical energy into heat and then dissipate it.<sup>[120]</sup> Similarly, mechanical and electrical systems lose energy in the form of heat. Although this heat dissipation is considered a loss, it creates energy harvesters, appropriately known as energy scavengers. Thermoelectric energy harvesters convert heat into electrical energy. It is through the association with MEMS technology that thermoelectric generators can be fabricated. The following section describes the principle of thermoelectric generation and outlines the recent progress of research into this form of energy harvesting. Different studies have investigated recent development in thermoelectric energy harvesters, with a focus on a specific aspect of thermoelectric harvesters, in terms of materials, designs, applications. The recent studies in this field are summarized in **Table 5**.

The vast majority of thermoelectric generators operate using the Seebeck effect. The Seebeck effect is defined as the generation of electric voltage as a result of a difference in temperature between two dissimilar conductors.

The Seebeck effect is the conversion of temperature differences straight into electricity. In the 1820s, Thomas Johann Seebeck realized that a compass needle would be deflected by a closed-loop formed by two different metals with a temperature difference between the junctions that joined in two places. This was because the metals reacted to the temperature difference in different methods, creating a current loop and a magnetic field.

In particular, the setup constituting the Seebeck effect is shown in **Figure 6A**, which shows the structure of what is known as a thermopile, the simplest manifestation of a thermoelectric generator using the Seebeck effect. Heat is applied to a tertiary conductor, which connects the two thermoelements, C1 and C2. Conversely, heat is removed from the opposite terminals of C1 and C2. The voltage generated through the Seebeck effect depends on the temperature difference between the hot and cold regions and material-dependent quantities and labelled Seebeck coefficients. Seebeck coefficients are a measure of the amount of voltage generated per unit of temperature difference. The direct relationship between these quantities and voltage is described in the following equation

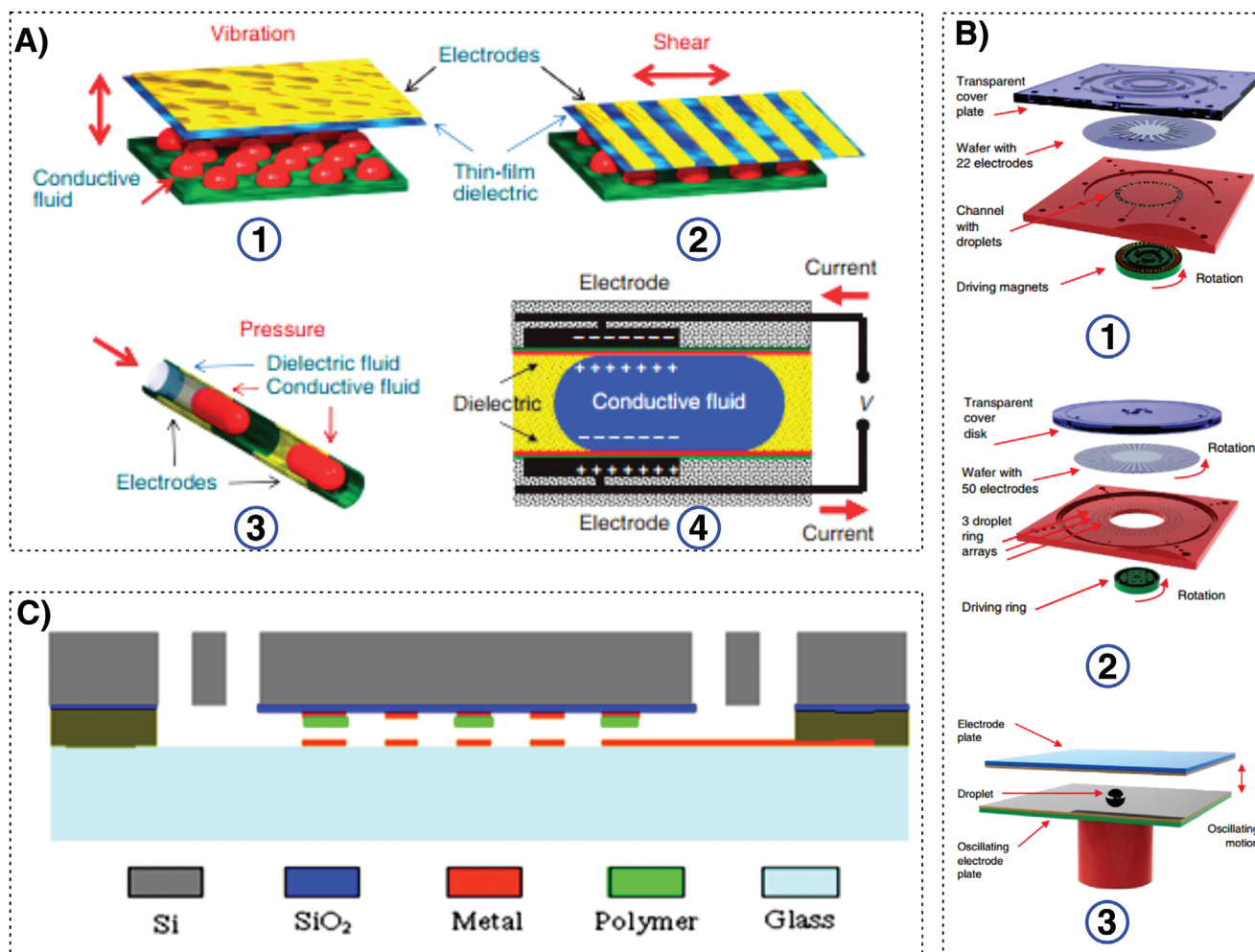


**Figure 5.** A) Reverse electrowetting process actuated by (1) out of the plane movement, (2) in plane shear movement, (3) pressurized droplet in channel movement, (4) illustration of the reverse electrowetting process. B) Various methods used for capacitance-based energy generation. (1) Magnet driven droplets in a microchannel. (2) In-plane shear movement. (3) Out of plane oscillation. Reproduced with permission.<sup>[118]</sup> Copyright 2011, Elsevier. C) Prototype of electrostatic harvester device. Reproduced with permission.<sup>[107]</sup> Copyright 2012, Springer Nature.

$$V = \int_{T_1}^{T_2} (a_{C_2}(T) - a_{C_1}(T)) dT \quad (6)$$

where  $V$  is the generated voltage,  $a$  is the Seebeck coefficient for a particular conductor, and  $T_1$  and  $T_2$  are the cold and hot temperatures, respectively.

It is commonly the case that the Seebeck coefficients are constant for a material; therefore, the equation can be simplified to the following

$$V = (a_{C_2} - a_{C_1}) \Delta T \quad (7)$$

In order to maximize the voltage produced, one would aim to improve two core areas. The first is in selecting or fabricating materials with polarized Seebeck coefficients. Semiconductors are used as the material for  $C_1$  and  $C_2$ . This is because semiconductors typically have high Seebeck coefficients, and doping a semiconductor in a particular way changes the polarity of the coefficient. Specifically, the Seebeck coefficients for an N-type and a P-type semiconductor are opposite

in sign,<sup>[131]</sup> constituting a high level of voltage generation. The second area requiring investigation is the creation of a higher temperature difference. This is generally achieved by applying different thermal sources, such as solar heating or combustion-based heating.<sup>[132]</sup> The microstructural arrangement of arrays of thermocouples, known as thermopiles, is also an important factor in improving efficiency; however, it is dependent on the application.

### 3.1. Recent Design Considerations

P-type and N-type are two different types of thermoelectric materials connected to form a thermocouple at one end. The ends of the thermocouple are placed in high and low temperatures, respectively. Because of the thermal excitation driving, the whole density of the P-type materials is higher than that of the low ones.

To attain a reasonable voltage at a low-temperature difference, single PN junction thermocouples should be placed in

**Table 5.** Recent studies on MEMS-based thermoelectric energy harvesters.

Reference	Year	Research focus	Recommendations
Rodriguez et al. <sup>[121]</sup>	2019	Application in automotive vehicles	<ul style="list-style-type: none"> <li>– The importance of integration with the heat exchangers and materials is referred.</li> <li>– The capability for direct and transitional waste heat recovery is depicted.</li> </ul>
Champier <sup>[122]</sup>	2017	Novel application	<ul style="list-style-type: none"> <li>– The application and design of thermoelectric generators in macro- and microscale is highlighted.</li> </ul>
Russ et al. <sup>[120]</sup>	2016	New material development	<ul style="list-style-type: none"> <li>– The capability of open-shell, stable radical polymers and molecules in terms of electronic structures, besides organic semiconductors, is represented.</li> <li>– Considered the flexibility and high ionic conductivity of some polymers.</li> </ul>
Junior et al. <sup>[123]</sup>	2018	Theory implementations	<ul style="list-style-type: none"> <li>– The importance of new materials discovery and the modification of the existing ones' crystalline structure via nanotechnology is described.</li> </ul>
Selvan et al. <sup>[124]</sup>	2018	Advanced design	<ul style="list-style-type: none"> <li>– Listed the improvements in bulk, thick, and thin-film thermoelectric generators.</li> <li>– Referred to the capabilities of recent achievements in thick and thin-film generators.</li> </ul>
Zhu et al. <sup>[125]</sup>	2015	Novel materials development	<ul style="list-style-type: none"> <li>– The need for further improvement in the performance of half-Heusler compounds in high-temperature power generation is illustrated.</li> </ul>
Guo and Lu <sup>[126]</sup>	2017	Novel application in pavements	<ul style="list-style-type: none"> <li>– The capacity of thermoelectric-based pipe systems regarding solar radiation maps is outlined.</li> </ul>
Twaha et al. <sup>[127]</sup>	2016	Mathematical modeling	<ul style="list-style-type: none"> <li>– The significance of advanced thermoelectric mathematical modeling is depicted.</li> </ul>
Li et al. <sup>[128]</sup>	2019	New wearable application	<ul style="list-style-type: none"> <li>– Listed the prototypes of thermoelectric generators based on the film- and fibre-based materials in wearable application.</li> </ul>
Yan et al. <sup>[129]</sup>	2018	Advanced material design and performance check	<ul style="list-style-type: none"> <li>– The importance of integrating thermoelectric generators to other harvesting techniques, e.g., solar cells, is highlighted.</li> </ul>

series for forming a thermoelectric module. Thermoelectric power generators are modules or groups of modules designed for obtaining electrical power from a heat source. Indeed, a single PN junction as new potential energy is very small. However, if many PN junctions are installed in series to form a thermopile, a high voltage can be produced. Therefore, an

energy collector capable of realizing hot spot conversion can be obtained.<sup>[133]</sup>

In recent years, there have been some cases of thermoelectric generators (TEGs) used for harnessing energy. The function of a TEG is to measure the temperature difference between its two sides and convert the temperature gradient into electric power.

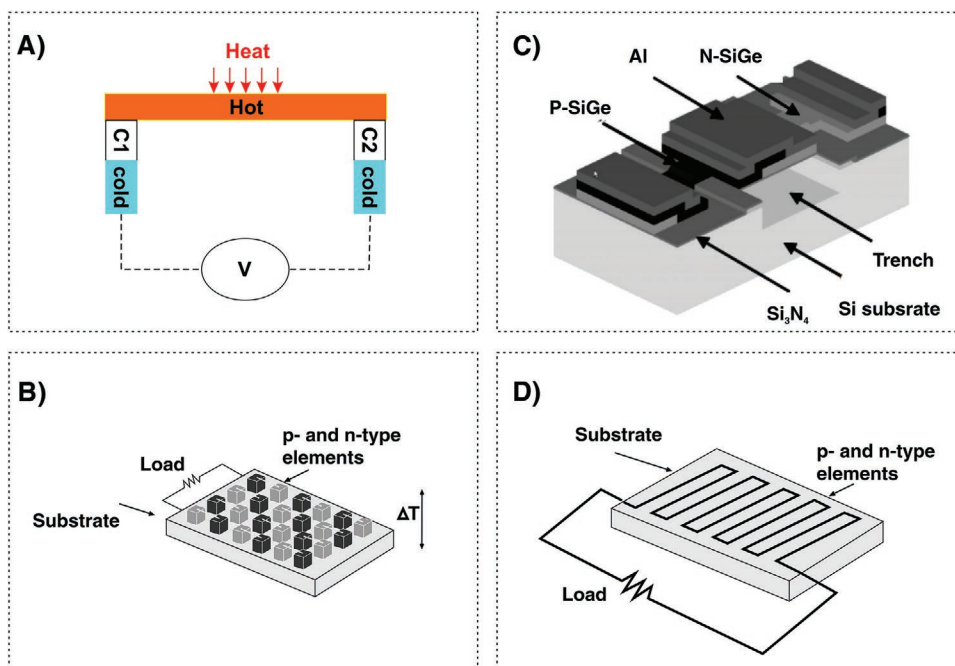


**Figure 6.** Fundamentals and structures of the thermoelectric energy harvesters. A) Illustration of the Seebeck effect. B) Schematic of poly-SiGe thermocouple, thermoelectric generator. C) the diagram of a through-plane thermoelectric module. Heat flow is crossing the plane of the substrate, which is parallel to the deposition direction. Reproduced with permission.<sup>[130]</sup> Copyright 2007, IEEE. D) the diagram of an in-plane thermoelectric module. Heat flow is in the Plane of the substrate, which is perpendicular to the deposition direction.

The output current depends on the size of the TEG and the temperature difference it holds. TEG is typically used in high-temperature environments, such as industrial heating systems, to power wireless sensor nodes. The TEG can be mounted between the power transistor and its heat sink to recover lost energy.<sup>[134,135]</sup>

Also, micro-thermoelectric energy collectors have been introduced. They are divided into two structures, vertical structure and planar structure. The vertical type of thermoelectric energy collector structure is firm, and the rate of temperature difference utilization is high. However, the production of vertical energy collectors is complex, so it is challenging to achieve low-cost mass production by vertical structure. In addition, the number of thermocouples per unit area is small, and the basic material is harmful to the human body. On the other hand, the planar thermoelectric energy collector has a floating structure. Due to this, the structure is fragile, but the reliability is poor.<sup>[129,136]</sup>

Using MEMS micromachining strategies, the costs of thermoelectric fabrication systems can be reduced. A strategy has been put forward to manufacture polycrystalline SiGe using the MEMS-based fabrication method.<sup>[130]</sup> Figure 6B shows a model of a single thermocouple capable of producing 1 V, featuring a 0.5  $\mu\text{m}$  high step and a 2.5  $\mu\text{m}$  deep trench. Also, research was conducted into the development of thermoelectric generator films using BiTe.<sup>[137]</sup> In regard to micro-thermoelectric generators created for industrial applications, some modifications for the generators are made depending on the heat source. Researchers have shown that the effectiveness of solar-based thermoelectric generators can be improved by using solar collector plates.<sup>[138,139]</sup>

### 3.2. Recent Fabrication Strategies

In order to exploit the thermal capabilities of solar heating, researchers developed thin-film thermoelectric modules which excel in the presence of focused solar light.<sup>[140]</sup> The film featured P- and N-type films, acting as Seebeck materials. Their selectivity was important since they had Seebeck coefficients of 150 and  $-104 \mu\text{V K}^{-1}$ , respectively, constituting a difference of  $254 \mu\text{V K}^{-1}$ . The novelty was the use of a cylindrical lens to focus the light of the sun, producing a 0.8 mm wide beam with the solar concentration of 12.5 suns (1 sun is equal to  $1 \text{ kW m}^{-2}$  of solar irradiance). The key technology in the fabrication of the module was lithography. However, although using solar energy to generate thermal energy is proving to be successful, it is sometimes unsuitable for indoor use.

A novel approach to generate heat for a micro-thermoelectric generator is catalytic combustion on a microscale.<sup>[132]</sup> The key feature of this research is the MEMS-based fabrication that took place to achieve catalytic combustion and facilitate the Seebeck effect. Silicon Nitride is the first used material that was coated on the top side of a silicon wafer. A KOH etch mask is then applied to the underside. Low-pressure chemical vapor deposition (LPCVD) is used to apply two layers of silicon-germanium (one P-type and the other N-type) in a particular pattern to serve as the dissimilar thermoelectric materials. The surface is then coated with tin nitride and platinum using E-beam deposition.

This is performed to create electrical contact. A channel is then etched using KOH, with a shadow mask, to facilitate the flow of the combustible fluid.

Most of the microfabricated devices are designed based on the concept of the flow of heat through the plane of the substrate, which is parallel to the deposition direction. A diagram of such through-plane devices is shown in Figure 6C. An alternative way to fabricate microscale thermoelectric devices is related to the length of the thermos-elements to be parallel to the substrate, as shown in Figure 6D. For such in-plane devices, the film thickness determines the thermos-element width. This allows for much higher aspect ratios, as done by Rowe et al.<sup>[141]</sup>

More thermocouples per unit area can be potentially achieved with the development of thin substrates and in-plane designs. This type of design is also compatible with alternative, and possibly low-cost, fabrication techniques such as screen printing.<sup>[142]</sup> In-plane designs are fundamentally different from through-plane designs, in which the substrate must either be removed or have low thermal and electrical conductivities since the substrate will be a thermal and electrical bridge parallel to the entire length of the thermoelectric leg. A substrate layer with high thermal conductivity will reduce the efficiency and decrease the temperature difference across the device.

Another in-plane micro-thermoelectric design was developed by Inayat et al.,<sup>[143]</sup> which differed from the general configuration because only one type of semiconductor was used. Aluminum strips connected the semiconductor elements in series by diagonally running from the hot side to the cold side. The aluminum strips were thin compared to the thermos-elements to prevent thermal shorting from the hot to the cold side. The researchers also used a thin silicon substrate to ensure a low thermal conductivity. The advantage of this system is its simplicity because it consists of one semiconductor material acting as both substrate and thermoelectric material.

Microfluidics technology has been adopted for MEMS applications. For instance, Koppa et al.<sup>[144]</sup> presented a method for the fabrication of a self-powered, highly sensitive thermoelectric microfluidic sensor to measure the heat produced by the interaction of ethanol with water. The method was capable of detecting small temperature differences without the need for external heat sources or heat sinks.

In another research report, Wojtas et al. designed and prototyped a multilayer fluidic packaging system capable of increasing the output power of micro thermoelectric generators. This was through combining the micro-thermoelectric energy harvester with a low pumping power microfluidic heat transfer system, which resulted in a substantial output power enhancement.<sup>[145]</sup>

Also, named capillary heat exchanger, microfluidics technology has been integrated into thermoelectric generators to enhance energy harvesting efficiency. Mathew et al.<sup>[146]</sup> designed a phase-changing MEMS-based capillary heat exchanger to be used in thermoelectric generators. They analyzed its performance both experimentally and theoretically. They suggested that by continuing the development of these capillary heat exchangers, thermoelectric generator performance can increase in many potential energy scavenging applications, one of which is in waste heat recovery, studied in ref. [7].



### 3.3. Practical Applications and Output Performance

The study of thermoelectric materials makes it possible to improve further the output performance of miniature hot spot energy collectors. The application prospect of micro-thermoelectric energy harvesters is broad and has important strategic significance to sustainable energy utilization.

Research has also been conducted on different sources of heating. It must be noted that although thermoelectric generators operate in any environment with ambient heating, the particular source of heating is mainly application-dependent. For example, thermoelectric generators operating outdoors are tailored to suit solar thermal energy collection.

The first application for MEMS-based thermoelectric generation, and certainly the most researched one, is on the human body, especially wearable systems. Motivated by the need for self-powering implantable and external electronics, researchers have investigated the use of human body heat as a source of energy. In 1999, a research paper was published that described the fabrication of a thermopile through electron discharge machining.<sup>[147]</sup> The generator was created for use in Seiko's watch line, offering customers a battery-free solution. It was recorded that the average voltage generated by the thermopile was 300 mV. During the next decade, with the rapid growth in MEMS, thermoelectric generators were created with higher voltage outputs, despite the decrease in size. In 2009 a research paper was published that described a wearable thermoelectric generator.<sup>[148]</sup> Micromachining was used to fabricate 4700 thermocouples on a chip. This device offered an open-circuit output voltage of 12.5 V ( $K^{-1} \text{ cm}^{-2}$ ) and an output power of  $0.026 \mu\text{W}$  ( $K^{-1} \text{ cm}^{-2}$ ).

An example of thermopile optimization for applications on the human body was reviewed in ref. [131]. To overcome the large thermal resistance of the skin of the human body, micromachined thermopiles were created in a rim structure. This has the benefit of increasing the thermal insulation of the thermopile.

Progress in human-based thermoelectric energy harvesting has been carried out in thermoelectric generators in fabrics. Researchers proposed printing 12 thermocouples in a polymer-based fabric connected with a conductive thread.<sup>[149]</sup> It was found that the device generated a power of 224 nW when used on the human body. Similarly, a jacket has been developed which harvests energy using the temperature difference between the human body and the ambient temperature.<sup>[150]</sup> However, it must be noted that the power generation was in the order of microwatts since there was a slight temperature difference.

Thermoelectric devices have been used in biomedical applications. A fully functional body-heat powered pulse oximeter has been presented in ref. [151]. The device uses a microscale thermoelectric generator mounted on a watch-like device for generating the necessary electrical energy. It also has the capability of transmitting data wirelessly. This is all achieved without the need for a battery, as it only contains a supercapacitor, which functions as an energy buffer. Research has been similarly conducted into self-powering implantable electronics as a thermoelectric generation for wearable electronics. MEMS-based bio-sensing technologies are becoming more famous due

to their small size, low power consumption, and high ability to be integrated.<sup>[152]</sup> Researchers have investigated the potential of implantable thermoelectric sensors for applications, including the measurement of glucose in the body.<sup>[153]</sup> Since this field is challenging, holding the possibility of side effects to patients, research was conducted into the practicality of implantable energy scavengers below the skin and fat layers.<sup>[154]</sup> This research determined the temperature gradient of a cross section of a part of the body, and experiments were performed when the thermoelectric generators were placed at a certain position in the body. Ultimately, the research article confirmed the practicality of implantable thermoelectric generators and created a valuable reference for designing such devices.

Additionally, thermoelectric materials are applied to microwave power sensors. Terminal MEMS microwave power sensor is divided into direct heating and indirect heating microwave power sensors. Directly heated microwave power sensor load is limited to 100 ohms, the load resistance is the thermocouple, so the conversion rate is swift. Indirect heating of the thermocouple and load resistance are separated; its efficiency and time constant are inferior to the self-heating type. However, the heated impedance matching design profile is more flexible than self-heating type wide.<sup>[155]</sup>

## 4. Radio-Frequency-Based Energy Harvesting

Over the past years, the power consumption of electronic devices and the use of batteries have been increasing, while the replacement of batteries is a tedious task in some situations, depending on feasibility and availability. Radiofrequency (RF) MEMS energy harvesting can be adapted to overcome the problem of supplying electrical energy. The RF MEMS device is fabricated on a chip, in which energy can be tapped easily and efficiently with increased scalability and high-performance factor.

By incorporating RF MEMS devices, there are multiple ways for energy harvesting. This system offers a reliable solution for self-powered microsystems. Its application range is from wireless network systems to portable electronic devices, widely used across the globe. By this technique, we capitalize on the free energy resources available in establishing maintenance as a free source throughout the system's lifetime. Since this is a budding area of study, many types of research and investigations are carried out to bring out a reliable, long-lasting solution for these problems.<sup>[156]</sup> Optimum and efficient fabrication and design schemes should be implemented. To achieve one full cycle of charge and discharge, it is essential to determine the pull-down voltage. Ideally, the pull-down voltage of the RF MEMS device was found to be 35V, and the energy discharge was 1 pF of capacitance. Hence, this computes to 2.18 electrons charged and discharged per cycle. Suitably choosing the type of photosensitive material enables a high energy conversion rate. Optimization of this design to store charge from pulsed charge and constant energy is still the scope of action.<sup>[157]</sup>

However, one of the challenging issues in RF MEMS devices is the electrostatic discharge-induced failure. The continuous charge and release of the electrons generated by the photosensitive layer in the RF MEMS device, commonly

**Table 6.** Recent studies reviewing MEMS-based radio-frequency energy harvesters.

Reference	Year	Research focus	Key contributions
Cansiz et al. <sup>[158]</sup>	2019	Efficiency enhancement	<ul style="list-style-type: none"> <li>– Highlighted the low power density of the RF energy harvesters.</li> <li>– Compared to other types of energy harvesters and depicted that RF energy harvesters produce sufficient energy to power up some sensors and/or devices.</li> <li>– Reviewed the performance of blocks of an RF energy harvesting circuit, i.e., antenna and matching circuit, rectifier, voltage multiplier, and energy storage device.</li> </ul>
Sherazi et al. <sup>[159]</sup>	2018	Application in powering wireless sensors	– Introduced the protocols for RF-based energy harvesting in wireless sensor networks.
Kaur et al. <sup>[160]</sup>	2018	Design and performance advancement	– The better performance with small size, better-occupied antenna space, better harmonic rejection and circular polarization are highlighted.
Dai et al. <sup>[161]</sup>	2015	Topology update	– The wide input range and capability to adjust the transistor size, as important factors, is depicted.
Selvan et al. <sup>[162]</sup>	2018	Application in powering wireless sensors	<ul style="list-style-type: none"> <li>– Summarized the recent development of RF energy harvesters.</li> <li>– Introduced the optimal designs for self-sustainable devices.</li> </ul>

known as electrostatic discharge induced loss, leads to reliability issues. This leads to the injection and trapping of charge in the gap between the insulation layer and metal owing to high electrical strength. The primary reason for this issue might occur during the fabrication process itself due to improper handling procedure or might occur due to induced charge. Continuous exposure to ESD will lead to deterioration of RF properties such as return signal losses, insertion losses, and loss of electromechanical properties up to the point where it reaches its critical value leading to total system failure. RF-based energy harvesters have been of interest to recent researchers. **Table 6** illustrates some of the recent papers reviewing different aspects of RF-based harvesters.

#### 4.1. Recent Design Considerations

The RF MEMS switches are used to modulate low-frequency electrical signals. These switches are more commonly adapted compared to conventional switches due to their advantages, such as low power consumption and fewer losses. Huang et al.<sup>[157]</sup> suggested a concept where MEMS switches can be used for energy harvesting. Capacitive membrane switches are

highly regarded as energy harvesting devices because of their high performance and high life expectancy, reaching about 1 billion cycles.

**Figure 7A**<sup>[160]</sup> shows that the RF MEMS switch is a coplanar waveguide shunt switch. The capacitive RF MEMS switch operates in two conditions when the thin layer (membrane) is in the top position (which is the normal state), it is considered as OFF condition, and subsequently, when the membrane is at the down position, the switch is said to be in ON condition. These two working conditions imply that when the switch is in the OFF state, there is a small, negligible value of capacitance, and when the switch is in the ON state, the high-value capacitor is grounded. Also, **Table 7** depicts the physical properties of the shown RF MEMS switch. The structure can be simplified as a 1D linear electromechanical model.

The Young's modulus of aluminum is 70 GPa,  $k = 133 \text{ N m}^{-1}$  from the equation, the  $V_p = 41 \text{ V}$ .

According to,<sup>[163]</sup> the spring constant is

$$k = 32Ew \left( \frac{t}{l} \right)^3 \quad (8)$$

where  $E$  is Young's modulus of the material,  $w$  is width,  $t$  is thickness, and  $l$  is length.

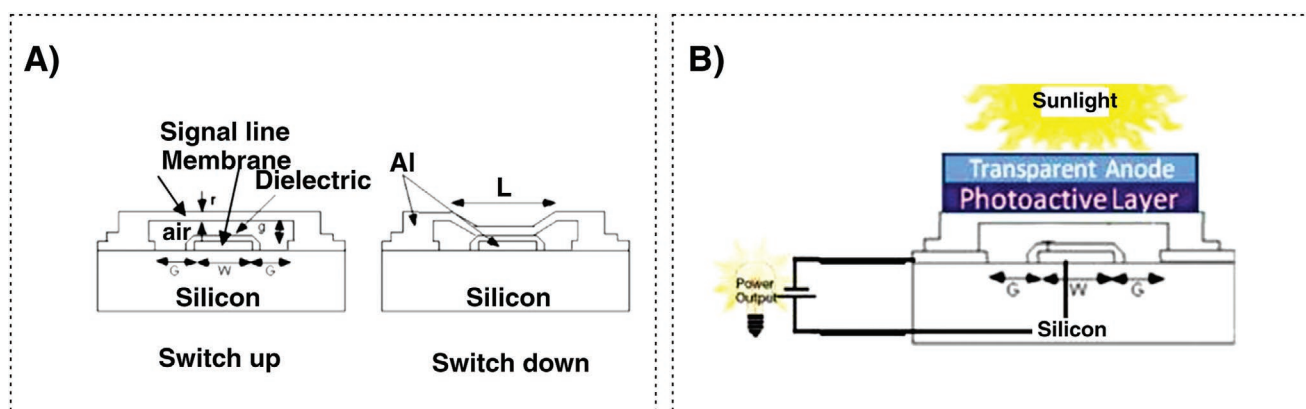


**Figure 7.** A) Schematic of RF MEMS switch. Reproduced with permission.<sup>[163]</sup> Copyright 2012, IEEE. B) Structure and functioning of RF MEMS device. Reproduced with permission.<sup>[157]</sup> Copyright 2010, IEEE.

**Table 7.** Dimensions of RF MEMS switch.<sup>[163]</sup>

Item	Material	Dimension
MEMS bridge	Al	$t = 1 \mu\text{m}$
		$l = 150 \mu\text{m}$
		$w = 200 \mu\text{m}$
Signal line	Al	$t = 1 \mu\text{m}$ $w = 100 \mu\text{m}$
Dielectric layer	SiO <sub>2</sub>	$g_{\text{SiO}_2} = 1 \mu\text{m}$
GSG gap	Air	$G = 25 \mu\text{m}$
Air gap	Air	$g_{\text{air}} = 1.7 \mu\text{m}$

The electrostatic force is evenly distributed across the membrane. The voltage between membrane and signal line leads to electrostatic force. To work out the approximately result of this force, the membrane is assumed to be a parallel-plate capacitor and the capacitance can be calculated as

$$C = \frac{\epsilon W w}{g} \quad (9)$$

where  $g$  is the height of the membrane and  $W$  is the width of the signal line.

The equation between electrostatic force and voltage is shown as

$$F_e = \frac{V^2}{2} \frac{dC(g)}{dg} = -\frac{\epsilon W w V^2}{2g^2} \quad (10)$$

As the electrostatic force is evenly distributed across the membrane, the deformation of spring can be used to determine the movement of the membrane under the applied force

$$V_p = \sqrt{\frac{8kg^3}{27\epsilon WL}} \quad (11)$$

where  $V_p$  is the pull-down voltage and  $g$  is the equivalent gap between membrane and signal line.

#### 4.2. Recent Fabrication Strategies

Many procedures were followed in the fabrication process of RF MEMS structures. One of the feasible and reliable methods involved depositing a thin aluminum layer on the substrate, which acts as a signal line. Aluminum is used in membrane fabrication, considering its low electrical resistance and high fatigue tolerance. In order to activate the RF MEMS switch capacitor while the membrane is pulled down, an insulating dielectric layer of silicon dioxide is deposited over the aluminum layer. Followed by this, another layer of member (aluminum) is deposited on the sacrificial layer, which is eventually released during the surface micromachining process. By doing so, the membrane is found to be in an ON state, which is essentially the original position of the switch. Upon applying a sufficient amount of dc voltage between the electrode and

membrane, the membrane moves down to its ON state. PECVD machine is used to deposit a thin dielectric layer, which separates the signal line from the membrane. Additionally, a protective layer of photoresist is coated on the MEMS structure post-fabrication to avoid damage during dicing and to provide protection from external contaminations. The details for fabrication are gathered in ref. [163].

#### 4.3. Practical Applications and Output Performance

In the last few decades, a gap between the power consumption of electronic devices and the electric capacity of onboard batteries has been growing. In some situations, such as wireless sensor networks, the replacement of batteries is usually not practical. Therefore, technologies of recharging the system when power is depleted have been in great demand. Absorbing energy from unlimited natural sources like solar and thermal power can solve this issue. However, the existing technologies like wind power harvesting have various technical barriers, needed to be solved.<sup>[164]</sup>

Thus, introducing an RF MEMS energy harvesting device is an essential solution for the replacement of onboard batteries. Moreover, the discontinuous charging process makes it possible for ions to redistribute evenly to different sizes of MEMS. These unique advantages contribute to greater scalability and higher efficiency for RF MEMS energy scavenging devices compared to other types of energy harvesters, which has become a hot spot in the field of MEMS since the 1990s.

This design technique enables the generation of charge when a photosensitive material is coated on the membrane, thereby replacing external voltage applied, which can be useful in the field of internet-of-things applications.<sup>[156]</sup> The charge is generated by a photosensitizing material stored in the gap between the signal line and the device's membrane. In a controlled condition, this generated charge can be stored in the RF device and further discharged to an external source or storage device in the form of pulsated energy (Figure 7B). Furthermore, by controlling the frequency of the RF device's ON/OFF mechanism, the output voltage can be adjusted. The maximum amount of energy stored in the device is influenced by membrane overlapping on the isolation layer. Considering the obtained capacitance under OFF and ON states, and by using experimental equation  $Q = C \times V$ , where  $Q$  is the charge,  $C$  is the capacitance, and  $V$  is the voltage, the maximum stored charge can be calculated.

### 5. Photo-Electrochemistry-Based Energy Harvesting

Approximately the power of  $1.8 \times 10^{11}$  MW of solar energy reaches the earth, making solar one of the most abundant sources of energy.<sup>[165]</sup> An added advantage of solar energy is that it is entirely renewable. These factors have combined to encourage the development of cheap and reliable technologies to harvest solar energy.

The majority of solar energy harvesting technologies involve the direct conversion of incident light to electricity via the

exploitation of phenomena such as the photovoltaic effect. Solar energy harvesting is a well-established industry with 40 GW of generation capacity installed globally as of 2010.<sup>[166]</sup> The vast majority of this capacity, however, consists of conventional, non-MEMS-based solar technologies such as monocrystalline and polycrystalline silicon cells (first-generation solar cells) and thin-film solar cells (second generation solar cells).<sup>[166]</sup> In recent years, much research effort has been devoted to developing third-generation solar cells such as those based on organic and polymer materials with low-cost fabrication procedures.<sup>[167]</sup>

As is the case in other industries such as medicine<sup>[168]</sup> and electronics,<sup>[169]</sup> MEMS-based technologies and techniques have begun to find applications in the solar industry.<sup>[170]</sup> MEMS-based technologies and methods enable the fabrication of millimeter-sized and microscale conventional solar cells and entirely new cell architectures such as 3D structured cells. However, even though these microscale devices promise to be effective, there are still limitations and complexities in manufacturing these harvesters.

This section will provide background information on each generation of solar cells and a summary of the application of MEMS-based technologies and fabrication techniques in each generation.

### 5.1. Recent Design Considerations

First-generation solar cells are the most widely used solar cells and are generally characterized as highly efficient and costly. The three most common types of first-generation solar cells, distinguished by the semiconductor material, are monocrystalline silicon, polycrystalline silicon, and crystalline gallium arsenide (GaAs).<sup>[171]</sup>

Monocrystalline solar cells are one of the most mature and well-established solar PV technologies. Although relatively expensive, commercially available monocrystalline silicon solar cells have high efficiencies ranging from 14% to 19%.<sup>[165]</sup> However, in a laboratory setting, the highest recorded efficiency under standard testing conditions is 25.0%.<sup>[149]</sup> Monocrystalline solar cells are manufactured by layering P-type and N-type doped crystalline silicon wafers to form large PN junctions.<sup>[171]</sup>

In recent times, much research effort has been invested into the development of solar cells with reduced quantities of monocrystalline silicon whilst maintaining high efficiencies.<sup>[172]</sup> Generally, these goals are achieved through the miniaturization of individual solar cells. In addition to lower costs, miniaturized solar cells find further applications in building-integrated photovoltaics and distributed sensor networks. Two approaches that have gained considerable attention amongst solar researchers are sliver cells and microsystem-enabled photovoltaic (MEPV) cells.

Developed by researchers at the Australian National University, sliver cells are long, narrow, and thin monocrystalline silicon solar cells fabricated from thin monocrystalline silicon wafers.<sup>[173]</sup> Dimensions of individual Sliver cells range from 50 to 120 mm long and 0.2 to 2 mm wide; thus, compared to conventional monocrystalline silicon cells, hundreds of sliver solar cells can be fabricated from a single wafer.<sup>[173]</sup> Fabrication of the sliver cells involves several micromachining techniques

used in the MEMS and integrated circuit industries, including photolithography, KOH etching, reactive ion etching (RIE), and plasma-enhanced chemical vapor deposition (PECVD).<sup>[173]</sup> Once fabricated, the individual cells are then assembled to form modules including tens to thousands of electrically connected sliver cells, as shown in **Figure 8A**.

The research team behind the development claims that this technique decreases silicon consumption by 10–15 times, corresponding to a reduction in wafers throughput per 1 MW of capacity manufactured by a factor of 20–50 when compared to conventional monocrystalline silicon solar cells.<sup>[177]</sup> In addition to these material reductions, sliver cells have some flexibility and are reported to have an efficiency of 19%.<sup>[178]</sup> Although some aspects of this approach are desirable, the major drawback is the lack of efficiently handling and assembling individual sliver cells into modules.<sup>[173]</sup>

MEPV cells, pioneered by Sandia National Laboratories, are another structure that reduces the amounts of monocrystalline silicon material required to fabricate solar cells. However, unlike sliver cells, this approach can be applied to other solar cell types, including GaAs cells. In the case of monocrystalline silicon, hexagonal cells down to 250  $\mu\text{m}$  in diameter and 20  $\mu\text{m}$  in thickness can be fabricated.<sup>[179]</sup>

### 5.2. Recent Fabrication Strategies

The fabrication of MEPV cells involves numerous microfabrication techniques common in the MEMS and integrated circuit industries on SOI wafers or oriented crystalline silicon wafers.<sup>[179]</sup> The process for fabrication of this type of solar cell is described in ref. [179]. Once fabricated in microscale, the cells are then transferred from the wafer to flexible films where they are interconnected to form modules. Figure 8B shows a flexible module, where a tip of a typical ball-point pen is included for scale. As of 2013, the highest achieved module efficiency was 13.75%, with a maximum power output of 21.8 mW.<sup>[174,180]</sup>

Polycrystalline silicon solar cells have the most influential global annual production rate. Although they are typically less efficient than monocrystalline silicon cells, polycrystalline silicon wafers are cheaper to manufacture due to the reduced temperatures required to manufacture polycrystalline silicon wafers.<sup>[181]</sup> However, an advantage that crystalline GaAs cells have over crystalline silicon cells is that they can be manufactured using thin-film technology with only a small decrease in efficiency.<sup>[171]</sup> GaAs solar cells have recorded an efficiency of 28.8% at optimum thickness, while thin-film GaAs solar cells are slightly lower at 26.4%.<sup>[44]</sup> GaAs is also highly resistant to heat and radiation, making them ideal for multijunction cells with solar concentrators.<sup>[171,182]</sup> The efficiency of GaAs solar cells may be raised to 29.1% with the use of a concentrator.<sup>[149]</sup>

Thin copper indium gallium selenide (CIGS) material also has a high photon absorption level, making it suitable for use in thin-film solar cells. The highest recorded efficiency in standard conditions is 21.0%.<sup>[149]</sup> An added feature of CIGS material is that it may be deposited effectively onto flexible substrates.<sup>[183]</sup> This feature enables the cells to be used in new applications such as building-integrated photovoltaics.<sup>[183]</sup>



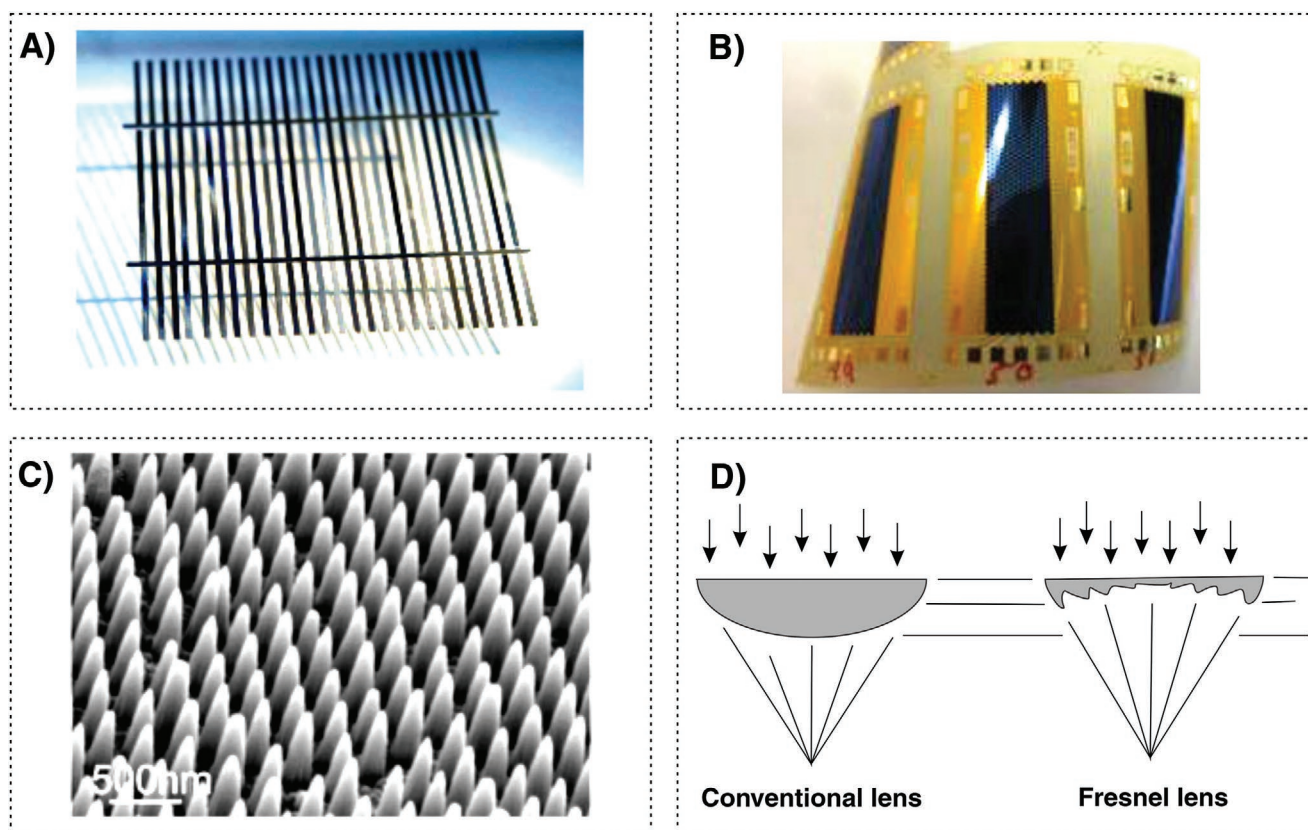


**Figure 8.** A) Small sliver cell module. Reproduced with permission.<sup>[172]</sup> Copyright 2007, Hindawi. B) Flexible MEPV solar cell mini-module. Reproduced with permission.<sup>[174]</sup> Copyright 2013, IEEE. C) Scanning electron microscope image of an amorphous silicon nanocone array. Reproduced with permission.<sup>[175]</sup> Copyright 2009, American Chemical Society. D) Comparison between conventional (left) and Fresnel (right) lenses. Adapted with permission.<sup>[176]</sup> Copyright 2005, Springer.

Amorphous (noncrystalline) silicon solar cells are amongst the most popular and well-developed thin-film solar cell technologies. The random arrangement of silicon atoms in an amorphous structure has a strong impact on the electrical properties of the material. Most significantly, amorphous silicon has a higher bandgap than crystalline silicon (1.7 eV compared to 1.1 eV<sup>[171]</sup>), resulting in visible light absorption more predominantly than infrared. The increased absorption of visible light makes amorphous silicon solar cells more suitable than bulk crystalline solar cells in indoor environments where infrared radiation is less abundant than visible light. As an example, amorphous silicon solar cells have been used in in-pocket and desk calculators since the 1980s.<sup>[184]</sup>

Third-generation solar cells are typically defined as those potentially able to overcome the Shockley–Queisser limit (the maximum theoretical efficiency of a PN junction solar cell<sup>[185]</sup>), which limits the performance of first and second-generation solar cell technologies.<sup>[171]</sup> The commercial readiness of these cell architectures ranges from the early stages of research and development to product demonstration.

Invented in 1991 O'Regan and Gratzel,<sup>[186]</sup> dye-sensitized solar cells (DSSCs) have quickly gained popularity amongst solar research groups due to their low cost and high efficiency compared to other third-generation solar cells. The highest recorded efficiency in standard conditions is 11.9%.<sup>[149]</sup> DSSCs do not convert

incident photons to electricity via light-absorbing semiconductors arranged in PN junctions like first and second-generation solar cells.<sup>[187]</sup> Instead, DSSCs are made up of an effective light-absorbing material such as a dye sensitizer, a wide bandgap semiconductor such as titanium dioxide.<sup>[187]</sup> These layers form a photo-electrochemical cell and are generally sandwiched between conducting glass materials. Incident photons are absorbed in the dye layer, generating electrons injected into the semiconductor layer and form electricity when connected to an external circuit. Electrons are subsequently given back to the dye layer from the electrolyte to reform the dye molecules. In the overall operation of the photo-electrochemical cell, electricity is generated without any permanent chemical changes.<sup>[187]</sup>

One variety of DSSC, which has gained significant research attention over recent years, is perovskite solar cells. Perovskite can be deposited from solution to form thin-film semiconducting layers.<sup>[188]</sup> A key attraction to perovskite for use in solar cells is the low-cost fabrication options such as roll-to-roll processing.<sup>[189]</sup> This technique requires much less energy compared to the fabrication of conventional silicon solar cells.

Organic solar cell materials have emerged as a low-cost and low-weight alternative to inorganic solar cell materials, including silicon, GaAs, CdTe, and CIGS. A significant feature of inorganic solar cells that researchers have identified is the prospect of very low-cost, rapid manufacturing procedures such

**Table 8.** Efficiencies of various multijunction solar cells.<sup>[149]</sup>

Type of multijunction cell	Efficiency (nonconcentrator) [%]	Efficiency (concentrator) [%]
Two-junction	31.1	34.1
Three-junction	37.9	44.4
Four-junction or more	38.8	44.7

as roll-to-roll processing.<sup>[167]</sup> With developments in semiconducting organic polymers, cell architectures have progressed from single organic layers with very low efficiencies to bulk heterojunction polymer-fullerene devices with laboratory efficiencies reaching 11.1%.<sup>[149]</sup> One of the major challenges limiting the commercialization opportunities of organic solar cells is their performance instability in operating conditions. Compared to their inorganic counterparts, organic materials are more prone to chemical and physical degradation.<sup>[189]</sup>

Quantum dots are nanoscale semiconductor crystals that exhibit heavily size-dependent optoelectrical properties.<sup>[190]</sup> In the context of solar cells, it is expected that the incorporation of quantum dots will increase photon absorption. Researchers are hopeful that this may enable the efficiencies of conventional Si-based cells to be raised above Shockley–Queisser limits.<sup>[189]</sup> In standard testing conditions, the highest achieved efficiency is 8.6%.<sup>[149]</sup>

Similar to quantum dots, semiconductor nanostructures have unique optical properties that have the potential to increase the photon absorption of solar cells.<sup>[175]</sup> In addition, these nanostructures may also increase the photo-carrier collection (collection of the free electrons generated by photon absorption), resulting in further cell efficiency increases.<sup>[189]</sup> Numerous semiconductor nanostructures, including nanowires, nanopillars, nanotubes, nanocones, nanospheres, and nanodomes, are being investigated to determine their performance in solar cell applications.<sup>[175]</sup> Fabrication of these nanostructures has been demonstrated with materials including crystalline silicon, amorphous silicon, cadmium telluride, and cadmium sulfide.<sup>[175]</sup> Figure 8C shows a scanning electron microscope image of an amorphous silicon nanocone array.

One method of increasing the efficiency of a solar module is to incorporate multiple PN junction layers into the module. By combining layers with a range of bandgaps, the total photon absorption of the module can be increased beyond the Shockley–Queisser limit of any of the individual layers.<sup>[191]</sup> However, a critical design consideration concerning the overall cell architecture is the current matching of each layer.<sup>[192]</sup> Differences between the current generated in each layer are significant contributors to overall cell inefficiency.

Although there is no limit in the number of junctions that can be incorporated into a multijunction solar cell, the efficiency gained for each additional layer diminishes as the total number of layers increases.<sup>[193]</sup> Beyond six junctions, the efficiency gained from adding further junction layers is minimal.<sup>[193]</sup> Multijunction cells are currently the most efficient solar cells developed. The highest recorded efficiencies of cells with two, three, and four or more junctions with and without concentrators under standard test conditions are summarized in **Table 8**.

Typically, multijunction solar cells are fabricated by depositing each of the semiconductor layers on top of the previous ones.

Challenges involved with this fabrication approach include the limited choice materials that are epitaxially compatible.<sup>[191]</sup> An alternative fabrication approach is to stack the layers mechanically. In 2014, Sheng et al. demonstrated a quadruple-junction solar cell fabricated via printing-based stacking of microscale solar cells.<sup>[194]</sup> The advantage of printing-based methods is that they can be rapidly scaled for high-throughput production.

As mentioned previously, solar concentrators are often used in conjunction with high-cost, high-efficiency solar cells such as multijunction cells to increase the intensity of light reaching the cell. In this way, the expensive solar cells can be reduced in size whilst still generating sufficient electricity. Practical concentration factors are generally no higher than 1000 suns as most solar cell materials degrade at the temperatures generated by higher solar concentrations. Concentrators can either be reflective surfaces or refractive lenses. The most common type of concentrator is a Fresnel lens which is a refractive lens.<sup>[176]</sup> Compared to traditional lenses, Fresnel lenses are compact and contain significantly less material – often polymers such as polymethylmethacrylate (PMMA) – making them much more lightweight.<sup>[176]</sup> In addition, the manufacturing processes for Fresnel lenses are well developed and low-cost.<sup>[176]</sup> A comparison between the shape of conventional lenses and Fresnel lenses is shown in Figure 8D.

Fresnel lenses make use of light refracted only at the interfacing surface between two transmission mediums. Since a conventional lens may be incorporated into a combination of prisms, each one represents a part of the slope of the traditional lens surface. Fresnel lenses for solar concentrator applications are typically fabricated with non-MEMS-based techniques, including injection molding.<sup>[176]</sup>

However, less common alternatives such as cylindrical concentrators can make use of MEMS-based fabrication techniques such as soft lithography. Yoon et al. investigated the fabrication of ultrathin silicon solar microcells with microconcentrators incorporated.<sup>[195]</sup> This group managed to boost the power output of their microcells by 2.5 with the addition of a polydimethylsiloxane (PDMS) microconcentrator fabricated via soft lithography.<sup>[195]</sup> Although concentrator photovoltaics (CPV) is a promising area being investigated, current issues slowing the commercial uptake of CPV systems include the additional costs involved with tracking and cooling systems.<sup>[165]</sup>

### 5.3. Practical Applications and Output Performance

Although DSSCs have received great attention over the past decade for their high energy conversion efficiency, relatively easy fabrication process, and low production cost, some practical difficulties such as solvent evaporation, leakage of liquid electrolyte, and sealing stability remain serious obstacles to convenient application. Therefore, a microfluidic DSSC housing system is proposed to assess the sealing performances of such architecture, which can be examined by fluid dynamic tests.<sup>[8,196]</sup>

Totally, the microfluidic approach for the fabrication of DSSCs is based on a reversible sealing of the two transparent electrodes, which allows the easy assembling and disassembling of the cell, making possible an analysis of the components over time. Using a microfluidic architecture makes it

possible to monitor the photo-anode and the counter electrode properties during their lifetime and perform a nondestructive analysis.<sup>[196]</sup> Also, microfluidics has been utilized in biosolar cells to improve biosolar cell performance. A miniature microfluidic-based single-chambered device is developed in this approach, which is different from the conventional, dual-chambered biosolar cells with a face-to-face electrode arrangement.<sup>[197,198]</sup>

For many solar power applications, high solar concentration is critically demanded to minimize the footprint size and effectively save the material cost of solar receivers. In one case, an arrayed microfluidic tunable prism panel is designed to enable wide solar tracking and high solar concentration and to minimize energy loss. The elimination of bulky mechanical tracking systems and the use of low-cost, lightweight, and silent microfluidic tracking systems will be ideally suited for rooftop usage in residential areas.<sup>[199]</sup>

## 6. Body Motion Energy Harvesting

Kinetic energy can be recognized as one of the most straightforward energy sources, which can derive from the body motion of humans. Deformation or vibration of a moving component in the human body can frequently produce kinetic energy. Operational principles can roughly classify kinetic microenergy harvesters. Acquiring kinetic energy by the motions of the human body is one of the most frequently used methods, such as walking and arm motion, which will be presented in the following content.

### 6.1. Recent Design Considerations

Kinetic energy harvesters can be designed in a way to harvest energy from walking. For this, a tiny and lightweight device is needed. A MEMS-based energy harvester can convert intermittent, bidirectional, low-speed, and high torque mechanical power into electricity. The typical knee joint harvesting process is shown in **Figure 9A**,<sup>[200]</sup> where the subject mass is 58 kg, walking speed about  $1.3 \text{ m s}^{-1}$ , and step frequency about 1.8 Hz. Also, mechanical power outputs in other conditions can be exhibited in very different patterns, depending on several parameters—including walking speed and the subject's mass.

Another way of harvesting kinetic energy is to derive energy from arm motion. Characteristics of daily arm motions, including arm stretching, phone picking-up, moving a spoon to eat etc., are listed in ref. [201], where three coordinate systems are made to present shoulder, elbow, and wrist separately. A display of 7 corresponding degrees of freedom is shown in **Figure 9B**.<sup>[201]</sup> The maximum angular acceleration happens at the wrist in *z*-direction in the motion of moving an object to waist level; on the other hand, the minimum angular acceleration happens at the shoulder in the *y*-direction in the motion of moving a spoon to eat.

### 6.2. Recent Fabrication Strategies

A major field that is full of opportunities for MEMS device applications is medical industry. There is an increasing trend

toward the need for devices required to function in diverse biological environments.<sup>[202]</sup> Common devices made from rigid materials are not well suited to functioning in situations requiring flexibility. The ability to stretch and vary in shape and size is essential for operating adequately in dynamic environments. Proposed applications for such a device include skin-worn substrates and implanted devices that conform to body movement.

In the last few years, a new branch of microfluidic technology has opened the door to devices that can be stretched and deformed without losing their functionality. As opposed to using solid wires, these devices can use low-temperature liquid metals, such as Gallium alloys, to perform as brilliant conductors housed in flexible polydimethylsiloxane (PDMS) microchannels.<sup>[203]</sup> These components are stretchable, twistable, and bendable without breaking internal connections.

Also, microfluidic technology can be used in many applications, including onboard bodily sensors, which can monitor health parameters and wirelessly transmit them to a computer for analysis.<sup>[6,204]</sup> They can also be programmed similar to field-programmable gate arrays (FPGAs) to be adapted to various applications.<sup>[205]</sup> For power supply, currently, they use bulky, inflexible batteries. Nevertheless, some novel approaches have been presented for energy generation, such as a microfluidic reactor.<sup>[206]</sup> The main focus is on energy harvesting from external sources, e.g., body motion, as the most practical solution.

Another useful application that is currently being developed for microfluidics-enabled energy harvesting is a device that uses residual energy from a person's steps. The energy that is currently wasted while walking or running can be harnessed and reused to power devices, such as music players and smartphones. This device uses a pumping mechanism combined with a series of electrode-lined microchannels, using similar principles discussed in.<sup>[118]</sup>

### 6.3. Practical Applications and Output Performance

Advances in miniaturization paved the way for tiny medical devices, but supplying power for surgical implants and instruments for physiological monitoring remains a challenge. Therefore, self-charging devices can harvest their energy from human body motion.<sup>[134]</sup> With the rapid development of wireless sensor networks embedded in the intelligent structure and wearable health monitoring, with low power consumption and independent working system, the demand for reliable, persistent, and environmentally friendly power supply technology is becoming increasingly intense.<sup>[207]</sup> Therefore, the rise of energy harvesting technology from the human body is an effective solution to these problems. The lifetime of this solution is theoretically determined by the lifetime of the electronics that make up the energy harvester. There is no additional energy consumption or emissions, making it a typical "green" technology. However, the three approaches for converting the human body mechanical energy into electrical energy generally are electromagnetic, piezoelectric and electrostatic.



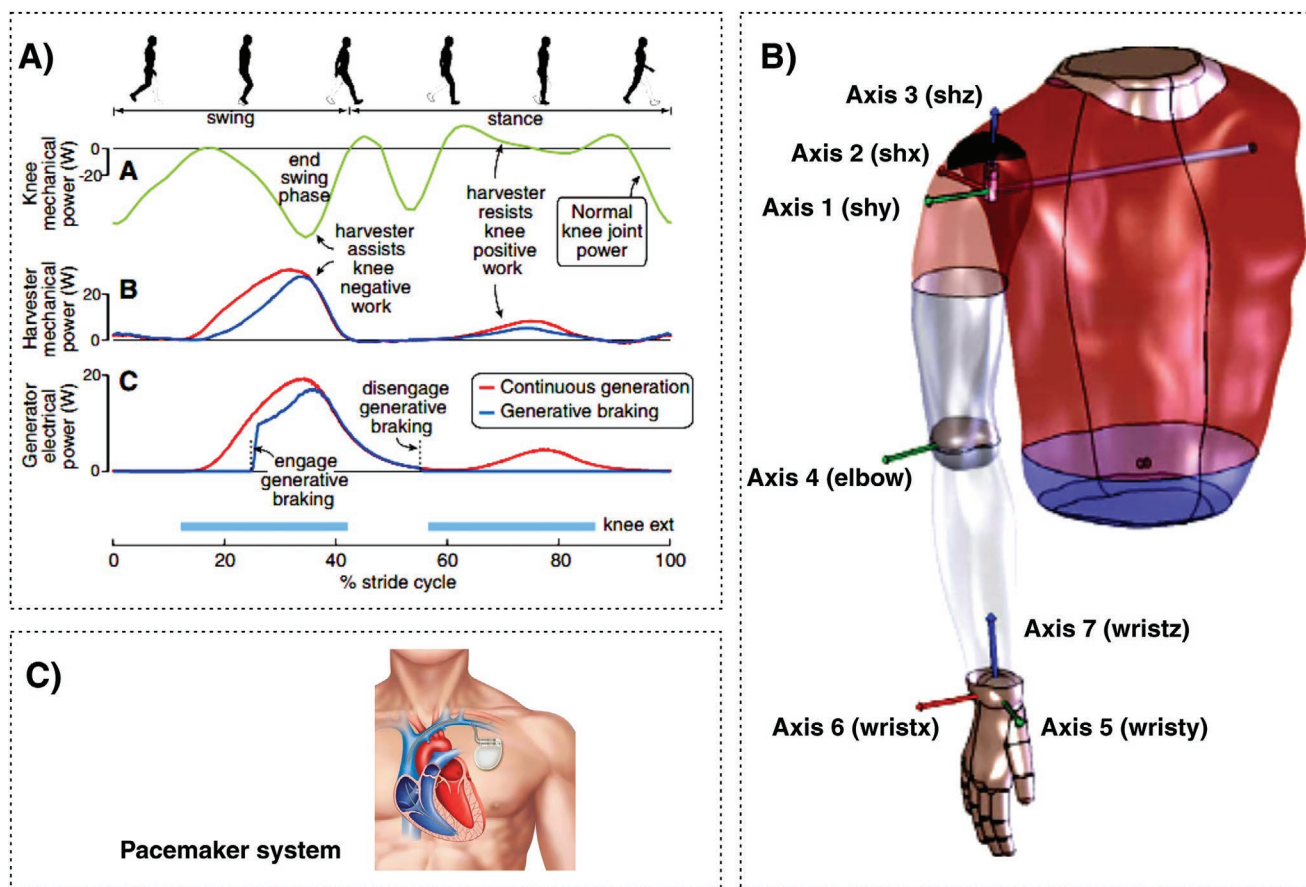


**Figure 9.** A) Timing of knee joint harvesting process. Reproduced with permission.<sup>[200]</sup> Copyright 2008, American Association for the Advancement of Science. B) Coordinate system of arm motions. Reproduced with permission.<sup>[201]</sup> Copyright 2005, IEEE. C) A self-powered pacemaker, being charged by the heart's own movement.

For example, a self-powered pacemaker, being charged by the heart's own movement, using an electromagnetic energy harvester, is proposed by researchers at Stanford University, as illustrated by Figure 9C.<sup>[134]</sup> The generator works when the heart muscle contraction causes the motion of a magnet in a conductor. It induces electric current running into the implanted pacemaker via electromagnetic effect. The pacemaker can receive more than 160  $\mu\text{W}$  of power, surpassing the energy needed to power the pacemaker.

## 7. Summary and Future Challenges

The increased demand for reliable and sustainable energy supply for microelectronic devices and ambient energy availability in our built environment has encouraged the development of energy harvesting technologies. Recent developments in MEMS and microfluidics have opened new ways to harvest ambient energy. In addition, MEMS-based fabrication techniques have enabled conventional energy harvesters to be shrunk to the microscale for integration to microelectronics. For instance, the advancement of microfabrication and microscale materials make the use of piezoelectric generators accessible for many applications. As such, MEMS systems can be readily integrated with polymer thin films or nanocomposite

piezoelectric substances. In this focused review, recent advances of the most prominent energy harvesting technologies such as piezoelectric, electromagnetic, electrostatic, thermoelectric, radiofrequency, and solar for self-driven micro/nanosystems are systematically summarized.

Some energy sources such as mechanical vibration are limited, but their applications are most widely found in almost all moving objects. By harnessing vibration energy, the energy harvesters can be used nearly anywhere and generate free energy. By using specific techniques, thermal energy can also be converted into electricity. Voltage is generated from the temperature gradient when heat transfers from the hot substance to the cool substance. As to RF-based energy harvesting, it works by rectifying a strong local signal aimed directly at sensors. Techniques in this field are in high demand for devices used in wireless sensor networks. Also, there is a need for small-scale electricity generation both in terms of power output and physical size for small-scale applications such as wireless sensor networks and IoT devices. In this regard, MEMS-based fabrication techniques are enabling suitable architectures to be developed, such as sliver solar cells, MEPV cells and printing-based multijunction microcells. In addition, MEMS-based fabrication techniques are enabling flexible solar cells that can find applications in building-integrated photovoltaics.



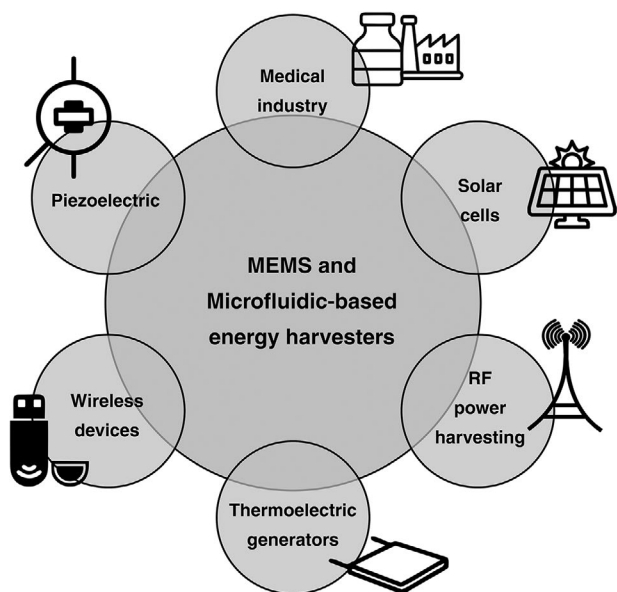


**Figure 10.** Key future application scopes of MEMS and microfluidics-based energy harvesters.

The concept of microfluidics is also being combined with other methods to scavenge ambient energies and convert them to electrical energy. Work is being done on the miniaturization of self-powered sensors, waste heat recovery, and electromagnetic devices, all incorporating microfluidic techniques to generate

or transfer energy.<sup>[170]</sup> Also, droplet-based energy harvesting systems have been recently developed as a substitute for bulky voltage sources in digital microfluidic systems.<sup>[208]</sup> Despite these microscaled devices showing promise to be effective, they are highly complicated and challenging to manufacture. Taking the vast scientific concepts and turning them into practical everyday devices is the goal of many scientists and engineers working in the MEMS/microfluidics field. Developing new ways to harvest energy is essential for these potentially mass-produced applications, shown in **Figure 10**. The area of microfluidics is positioned to play a vital role in this development due to its ability to make a way to create flexible energy harvesting devices that can be used in everyday activities. The future roadmap (**Figure 11**) depicts that advanced technologies will lead MEMS and microfluidics-based energy harvesters to be used for nerve cell stimulation and implanted for self-regulated drug delivery.

Striving toward the advancement of MEMS and microfluidics-based self-sufficient micro/nanosystems and their prospects, the following challenges should be resolved, requiring extra attention and efforts.

- I. Cost-effective, durable, and sustainable operation of energy harvesters is essential and requires further investigations.
- II. Biodegradability and biocompatibility issues of the energy harvesting materials is challenging for the safe and secure applications inside the body.
- III. Optimization of energy scavenging and converting capability, using appropriate fabricating materials and device structures, requires reliable and efficient operations.

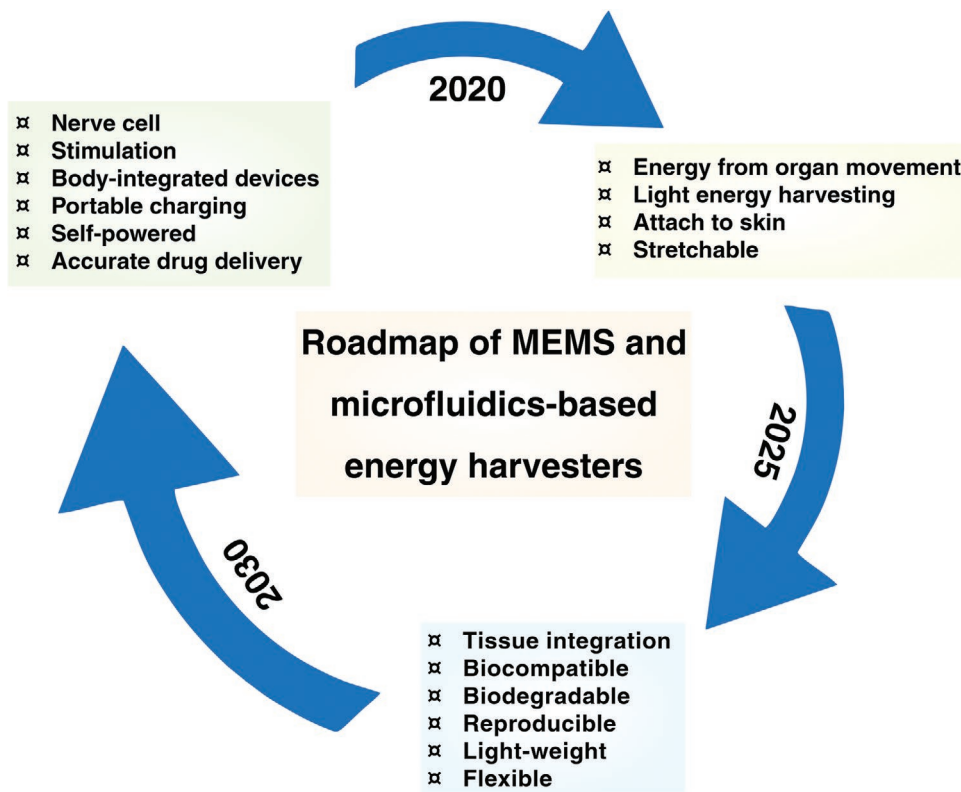


**Figure 11.** The future roadmap of MEMS and microfluidics-based energy harvesters.

- IV. Implementations of the newly developed energy harvesting devices are required to apply in large animals to justify the applicability in human for commercialization in the near future.
- V. Miniaturization of the energy harvesters remains a challenge for the infinite possibilities to apply in tiny bio-medical devices/surgical implants and devices for internal physiological monitoring.
- VI. Further studies and consideration are required for in vivo studies of energy harvesting systems in order to promote their clinical potential.
- VII. Better integration of artificial intelligence and big data with energy harvesting systems to assist in the analysis and design of these systems
- VIII. Development of hybrid energy harvesting systems to scavenge energy in a variety of forms.

## Acknowledgements

M.A.P.M. and S.R.B. contributed equally to this work.

## Conflict of Interest

The authors declare no conflict of interest.

## Keywords

energy harvesting, MEMS, micro/nanosystems, microfluidics

Received: October 13, 2021

Published online:

- [1] H. Madinei, H. Haddad Khodaparast, M. I. Friswell, S. Adhikari, *Energy* **2018**, 149, 990.
- [2] M. Han, Q. Yuan, X. Sun, H. Zhang, *J. Microelectromech. Syst.* **2014**, 23, 204.
- [3] B. Gale, A. Jafek, C. Lambert, B. Goenner, H. Moghimifam, U. Nze, S. Kamarapu, *Inventions* **2018**, 3, 60.
- [4] D. Thuau, C. Laval, I. Dufour, P. Poulin, C. Ayela, J.-B. Salmon, *Microsyst. Nanoeng.* **2018**, 4, 15.
- [5] Y. Wang, L. Wang, M. Yan, S. Dong, J. Hao, *ACS Appl. Mater. Interfaces* **2017**, 9, 28185.
- [6] X.u Li, D. R. Ballerini, W. Shen, *Biomicrofluidics* **2012**, 6, 011301.
- [7] N. Z. Wojtas, *Microfluidic Thermolectric Heat Exchangers for Low-Temperature Waste Heat Recovery*, ETH Zurich, xxxx **2014**.
- [8] C. Zhao, J. Zhang, Y. Hu, N. Robertson, P. A.n Hu, D. Child, D. Gibson, Y. Q. Fu, *Sci. Rep.* **2015**, 5, 17750.
- [9] S. Roundy, P. K. Wright, J. Rabaey, *Comput. Commun.* **2003**, 26, 1131.
- [10] J. Smilek, Z. Hadas, J. Vetiska, S. Beeby, *Mech. Syst. Signal Process.* **2019**, 125, 215.
- [11] C. Wei, X. Jing, *Renewable Sustainable Energy Rev.* **2017**, 74, 1.
- [12] Y. Suzuki, *IEEJ Trans. Electr. Electron. Eng.* **2011**, 6, 101.
- [13] W. G. Cady, *Piezoelectricity: Volume Two*, Courier Dover Publications, Mineola, New York **2018**.
- [14] J. Briscoe, S. Dunn, *Nano Energy* **2015**, 14, 15.
- [15] F. Ali, W. Raza, X. Li, H. Gul, K.i-H. Kim, *Nano Energy* **2019**, 879.
- [16] J. M. Mccarthy, S. Watkins, A. Deivasigamani, S. J. John, *J. Sound Vib.* **2016**, 361, 355.
- [17] J.-Y. Chang, *IEEE Trans. Magn.* **2011**, 47, 1862.
- [18] M. Aramaki, K. Izumi, T. Yoshimura, S. Murakami, N. Fujimura, in *2017 IEEE 30th International Conference on Micro Electro Mechanical Systems (MEMS)*, IEEE, Piscataway, NJ **2017**.
- [19] H.-C. Song, P. Kumar, D. Maurya, M.-G. Kang, W. T. Reynolds, D.-Y. Jeong, C.-Y. Kang, S. Priya, *J. Microelectromech. Syst.* **2017**, 26, 1226.
- [20] M. T. Todaro, F. Guido, V. Mastronardi, D. Denis, G. Epifani, L. Algeri, M. De Vittorio, *Microelectron. Eng.* **2017**, 23, 183.
- [21] E. Häsler, L. Stein, G. Harbauer, *Ferroelectrics* **1984**, 60, 277.
- [22] M. Umeda, K. Nakamura, S. Ueha, *Jpn. J. Appl. Phys.* **1997**, 36, 3146.
- [23] N. G. Elvin, A. A. Elvin, M. Spector, *Smart Mater. Struct.* **2001**, 10, 293.
- [24] H. A. Sodano, G. Park, D. J. Leo, D. J. Inman, *Proc. SPIE* 5050, 2003, 101.
- [25] G. K. Ottman, H. F. Hofmann, A. C. Bhatt, G. A. Lesieutre, *IEEE Trans. Power Electron.* **2002**, 17, 669.
- [26] G. K. Ottman, H. F. Hofmann, G. A. Lesieutre, *IEEE Trans. Power Electron.* **2003**, 18, 696.
- [27] S. Azizi, A. Ghodsi, H. Jafari, M. R. Ghazavi, *Energy* **2016**, 96, 495.
- [28] P. Pillatsch, B. L. Xiao, N. Shashoua, H. M. Gramling, E. M. Yeatman, P. K. Wright, *Smart Mater. Struct.* **2017**, 26, 035046.
- [29] A. Khan, Z. Abas, H. Soo Kim, I.I-K. Oh, *Smart Mater. Struct.* **2016**, 25, 053002.
- [30] S. Priya, H.-C. Song, Y. Zhou, R. Varghese, A. Chopra, S.-G. Kim, I. Kanno, L. Wu, D. S. Ha, J. Ryu, R. G. Polcawich, *Energy Harvest. Syst.* **2017**, 4, 3.
- [31] F. Narita, M. Fox, *Adv. Eng. Mater.* **2018**, 20, 1700743.
- [32] A. Abdelkefi, *Int. J. Eng. Sci.* **2016**, 100, 112.
- [33] T. Yildirim, M. H. Ghayesh, W. Li, G. Alici, *Renewable Sustainable Energy Rev.* **2017**, 71, 435.
- [34] N. X. Yan, A. A. Basari, K. S. Leong, N. A. A. Nawir, *J. Telecommun., Electron. Comput. Eng. (JTEC)* **2019**, 11, 35.
- [35] H. Elahi, M. Eugeni, P. Gaudenzi, *Energies* **2018**, 11, 1850.
- [36] N. Sezer, M. Koç, *Nano Energy* **2021**, 80, 105567.
- [37] H. A. Sodano, D. J. Inman, G. Park, *Shock Vib. Digest* **2004**, 36, 197.
- [38] H. S. Kim, J.-H. Kim, J. Kim, *Int. J. Precis. Eng. Manuf.* **2011**, 12, 1129.
- [39] E. Minazara, D. Vasic, F. Costa, in *Proc. Int. Conf. on Renewable Energies and Power Quality (ICREPO'08)*, Cambridge Scholars Publishing, Santander, Spain **2008**.
- [40] S.-G. Kim, S. Priya, I. Kanno, *MRS Bull.* **2012**, 37, 1039.
- [41] H. Liu, C. Quan, C. J. Tay, T. Kobayashi, C. Lee, *Phys. Procedia* **2011**, 19, 129.
- [42] R. Calìò, U. Rongala, D. Camboni, M. Milazzo, C. Stefanini, G. De Petris, C. Oddo, *Sensors* **2014**, 14, 4755.
- [43] M. E. Lines, A. M. Glass, *Principles and Applications of Ferroelectrics and Related Materials*, Oxford University Press, Oxford **2001**.
- [44] S. Priya, *J. Electroceram.* **2007**, 19, 167.
- [45] S. Roundy, P. K. Wright, *Smart Mater. Struct.* **2004**, 13, 1131.
- [46] H.-B. Fang, J.-Q. Liu, Z.-Y.i Xu, L.u Dong, L.i Wang, D.i Chen, B.-C. Cai, Y. Liu, *Microelectron. J.* **2006**, 37, 1280.
- [47] M. S. Bhuyan, M. Othman, S. H. M.d Ali, B. Y. Majlis, M.d.S. Islam, *Asian J. Sci. Res.* **2013**, 6, 1.
- [48] H. W. Kim, S. Priya, K. Uchino, R. E. Newnham, *J. Electroceram.* **2005**, 15, 27.
- [49] X. Li, M. Guo, S. Dong, *IEEE Trans. Ultrason., Ferroelectr., Freq. Control* **2011**, 58.
- [50] S.-J. Jeong, M.-S. Kim, D.-S.u Lee, J.-S. Song, *Integr. Ferroelectr.* **2008**, 98, 208.
- [51] S. Adhikari, M. I. Friswell, D. J. Inman, *Smart Mater. Struct.* **2009**, 18, 115005.
- [52] E. Lefeuvre, A. Badel, C. Richard, L. Petit, D. Guyomar, *Sens. Actuators, A* **2006**, 126, 405.
- [53] M. Lallart, P.-J. Cottinet, L. Lebrun, B. Guiffard, D. Guyomar, *J. Appl. Phys.* **2010**, 108, 034901.

- [54] I. Patel, E. Siores, T. Shah, *Sens. Actuators, A* **2010**, 159, 213.
- [55] N. Chapman, B. Chavero, M. Cross, D. Li, K. McLennan, R. Gamadia, *Piezoelectric Energy Harvesting with 3D-Printed Light-Up Shoe*, New Jersey Governor's School of Engineering and Technology, xxxx **2017**.
- [56] N. Han, D. Zhao, J. U. Schluter, E. S. Goh, H.e Zhao, X. Jin, *Appl. Energy* **2016**, 178, 672.
- [57] S. Bodkhe, G. Turcot, F. P. Gosselin, D. Therriault, *ACS Appl. Mater. Interfaces* **2017**, 9, 20833.
- [58] K. Kim, W. Zhu, X. Qu, C. Aaronson, W. R. Mccall, S. Chen, D. J. Sirbuly, *ACS Nano* **2014**, 8, 9799.
- [59] Z. Chen, X. Song, L. Lei, X. Chen, C. Fei, C. T. Chiu, X. Qian, T. Ma, Y. Yang, K. Shung, Y. Chen, Q. Zhou, *Nano Energy* **2016**, 27, 78.
- [60] T. Zawada, K. Hansen, R. Lou-Moeller, E. Ringgaard, T. Pedersen, E. V. Thomsen, *Proc. Eng.* **2010**, 5, 1164.
- [61] M. Marzencki, M. Defosseux, S. Basrour, *J. Microelectromech. Syst.* **2009**, 18, 1444.
- [62] L. Li, J. Xu, J. Liu, F. Gao, *Adv. Compos. Hybrid Mater.* **2018**, 1, 1.
- [63] W.-S. Jung, Y.-H.o Do, M.-G. Kang, C.-Y. Kang, *Curr. Appl. Phys.* **2013**, 13, S131.
- [64] H. K. Baik, *Google Patents*, **2018**.
- [65] Z. Wang, X. Pan, Y. He, Y. Hu, H. Gu, Y. Wang, *Adv. Mater. Sci. Eng.* **2015**, 2015, 165631.
- [66] G. Zhao, X. Zhang, X. Cui, S. Wang, Z. Liu, L. Deng, A. Qi, X. Qiao, L. Li, C. Pan, Y. Zhang, L. Li, *ACS Appl. Mater. Interfaces* **2018**, 10, 15855.
- [67] Z. Yangzhou, Y. Weifeng, Z. Chaoyang, G.u Bin, H.u Ning, *Mater. Res. Express* **2018**, 5, 105506.
- [68] S. Almsberger, K. V. Keppel, *Google Patents*, **2018**.
- [69] Y. Modi, *Google Patents*, **2016**.
- [70] B. Montaron, *Google Patents*, **1983**.
- [71] A. Wakabayashi, T. Tanabe, K. Hashimoto, *Google Patents*, **2018**.
- [72] C.-W. Chou, Y.-N. Cheng, *Google Patents*, **2006**.
- [73] X. Xu, D. Cao, H. Yang, M. He, *Int. J. Pavement Res. Technol.* **2018**, 11, 388.
- [74] J. Zhu, H. Wang, *IET Micro Nano Lett.* **2018**, 13, 1421.
- [75] T. Zhang, T. Yang, M. Zhang, C. R. Bowen, Y. Yang, *iScience* **2020**, 23, 101689.
- [76] Y. Tan, Y. Dong, X. Wang, *J. Microelectromech. Syst.* **2017**, 26, 1.
- [77] Z. Zergoune, N. Kacem, N. Bouhaddi, *Smart Mater. Struct.* **2019**, 28, 07LT02.
- [78] S. Naifar, S. Bradai, C. Viehweger, O. Kanoun, *Measurement* **2017**, 106, 251.
- [79] M. Q. Le, J.-F. Capsal, M. Lallart, Y. Hebrard, A. Van Der Ham, N. Reffe, L. Geynet, P.-J. Cottinet, *Prog. Aerospace Sci.* **2015**, 79, 147.
- [80] A. R. M. Siddique, S. Mahmud, B. V. Heyst, *Energy Convers. Manage.* **2015**, 106, 728.
- [81] H. Wang, A. Jasim, X. Chen, *Appl. Energy* **2018**, 212, 1083.
- [82] J. Choi, I. Jung, C.-Y. Kang, *Nano Energy* **2019**, 56, 169.
- [83] P. Miao, P. D. Mitcheson, A. S. Holmes, E. M. Yeatman, T. C. Green, B. H. Stark, *Microsys. Technol.* **2006**, 12, 1079.
- [84] C. B. Williams, R. B. Yates, *Sens. Actuators, A* **1996**, 52, 8.
- [85] N. N. H. Ching, H. Y. Wong, W. J. Li, P. H. W. Leong, Z. Wen, *Sens. Actuators, A* **2002**, 97, 685.
- [86] C. R. Saha, T. O'donnell, H. Loder, S. Beeby, J. Tudor, *IEEE Trans. Magn.* **2006**, 42, 3509.
- [87] S. P. Beeby, R. N. Torah, M. J. Tudor, P. Glynne-Jones, T. O'donnell, C. R. Saha, S. Roy, *J. Micromech. Microeng.* **2007**, 17, 1257.
- [88] P.-H. Wang, X.u-H. Dai, D.-M. Fang, X.-L. Zhao, *Microelectron. J.* **2007**, 38, 1175.
- [89] D. Zhu, S. Roberts, M. J. Tudor, S. P. Beeby, *Sens. Actuators, A* **2010**, 158, 284.
- [90] S. Turkyilmaz, H. Kulah, A. Muhtaroglu, in *2010 Int. Conf. on Energy Aware Computing (ICEAC)*, IEEE, Piscataway, NJ **2010**.
- [91] A. Rahimi, O. Zorlu, A. Muhtaroglu, H. Kulah, *IEEE Sens. J.* **2012**, 12, 2287.
- [92] Z. Xu, X. Shan, D. Chen, T. Xie, *Appl. Sci.* **2016**, 6, 10.
- [93] S. Sun, X. Dai, Y. Sun, X. Xiang, G. Ding, X. Zhao, *J. Micromech. Microeng.* **2017**, 27, 115007.
- [94] U. Radhakrishna, P. Riehl, N. Desai, P. Nadeau, Y. Yang, A. Shin, J. H. Lang, A. P. Chandrakasan, in *2018 IEEE Custom Integrated Circuits Conference (CICC)*, IEEE, Piscataway, NJ **2018**.
- [95] K. Tao, L. H. Tang, J. Wu, J. M. Miao, in *2018 IEEE 8th International Nanoelectronics Conferences (INEC)*, IEEE, Piscataway, NJ **2018**.
- [96] M. Rahman, R. Atkin, H. Kim, *J. Phys.: Conf. Ser.* **2015**, IOP Publishing, Bristol, UK.
- [97] H. Liu, Y. Qian, C. Lee, *Sens. Actuators, A* **2013**, 204, 37.
- [98] T. Krupenkin, J. A. Taylor, *Google Patents*, **2015**.
- [99] K. Najafi, in *Proc. of the 2000 Int. Symp. on Low Power Electronics and Design*, ACM, NY **2000**.
- [100] T. Sterken, K. Baert, C. Vanhoof, R. Puers, G. Borghs, in *Proc. of IEEE on Sensors, 2004*, **2004**, IEEE, Piscataway, NJ.
- [101] D. A. Barkas, C. S. Psomopoulos, P. Papageorgas, K. Kalkanis, D. Piromalis, A. Mouratidis, *Energy Procedia* **2019**, 157, 999.
- [102] H. Honma, H. Mitsuya, G. Hashiguchi, H. Fujita, H. Toshiyoshi, *J. Micromech. Microeng.* **2018**, 28, 064005.
- [103] C. Wu, A. C. Wang, W. Ding, H. Guo, Z. L. Wang, *Adv. Energy Mater.* **2019**, 9, 1802906.
- [104] W. Kim, D. Bhatia, S. Jeong, D. Choi, *Nano Energy* **2019**, 56, 307.
- [105] J. Yang, *An Introduction to the Theory of Piezoelectricity*, Vol. 9, Springer Science & Business Media, Berlin **2004**.
- [106] N.-C. Tsai, C.-Y. Sue, *Sens. Actuators, A* **2007**, 134, 555.
- [107] M. Triches, F. Wang, A. Crovetto, A. Lei, Q. You, X. Zhang, O. Hansen, *Proc. Eng.* **2012**, 47, 770.
- [108] F.-R.u Fan, Z.-Q. Tian, Z. Lin Wang, *Nano Energy* **2012**, 1, 328.
- [109] G. Zhu, B. Peng, J. Chen, Q. Jing, Z. Lin Wang, *Nano Energy* **2015**, 14, 126.
- [110] Y. Lee, S. H. Cha, Y.-W. Kim, D. Choi, J.-Y. Sun, *Nat. Commun.* **2018**, 9, 1804.
- [111] Y. Zi, S. Niu, J. Wang, Z. Wen, W. Tang, Z. L. Wang, *Nat. Commun.* **2015**, 6, 8376.
- [112] S. Pan, Z. Zhang, *J. Appl. Phys.* **2017**, 122, 144302.
- [113] X. Zhao, *Soft Matter* **2014**, 10, 672.
- [114] W. Xu, L.-B. Huang, M.-C. Wong, Li Chen, G. Bai, J. Hao, *Adv. Energy Mater.* **2017**, 7, 1601529.
- [115] G. Suo, Y. Yu, Z. Zhang, S. Wang, P. Zhao, J. Li, X. Wang, *ACS Appl. Mater. Interfaces* **2016**, 8, 34335.
- [116] P. Jiao, *Nano Energy* **2021**, 88, 106227.
- [117] E. Yildirim, H. Kulah, *Microfluid. Nanofluid.* **2012**, 13, 107.
- [118] T. Krupenkin, J. A. Taylor, *Nat. Commun.* **2011**, 2, 448.
- [119] S. Meninger, J. O. Mur-Miranda, R. Amirtharajah, A. Chandrakasan, J. H. Lang, *IEEE Trans. Very Large Scale Integ. (VLSI) Syst.* **2001**, 9, 64.
- [120] B. Russ, A. Glaudell, J. J. Urban, M. L. Chabiny, R. A. Segalman, *Nat. Rev. Mater.*, **2016**, 1, 16050.
- [121] R. Rodriguez, M. Preindl, J. S. Cotton, A. Emadi, *IEEE Trans. Veh. Technol.* 5366, **2019**.
- [122] D. Champier, *Energy Convers. Manage.* **2017**, 140, 167.
- [123] O. H. Ando Junior, A. L. O. Maran, N. C. Henao, *Renewable Sustainable Energy Rev.* **2018**, 91, 376.
- [124] K. V. Selvan, M.d N. Hasan, M. S. Mohamed Ali, *Int. J. Energy Res.* **2019**, 43, 113.
- [125] T. Zhu, C. Fu, H. Xie, Y. Liu, X. Zhao, *Adv. Energy Mater.* **2015**, 5, p. 1500588.
- [126] L. Guo, Q. Lu, *Renewable Sustainable Energy Rev.* **2017**, 72, 761.
- [127] S. Twaha, J. Zhu, Y. Yan, B.o Li, *Renewable Sustainable Energy Rev.* **2016**, 65, 698.
- [128] C. Li, F. Jiang, C. Liu, P. Liu, J. Xu, *Appl. Mater. Today* **2019**, 15, 543.
- [129] J. Yan, X. Liao, D. Yan, Y. Chen, *J. Microelectromech. Syst.* **2018**, 27, 1.
- [130] V. Leonov, R. Vullers, in *Proceedings of the 5th European Conference on Thermoelectrics (ECT)*, xxxx, Odessa, Ukraine **2007**.

- [131] R. J. M. Vullers, R. Van Schaijk, I. Doms, C. Van Hoof, R. Mertens, *Solid-State Electron.* **2009**, 53, 684.
- [132] S. B. Schaevitz, A. J. Franz, K. F. Jensen, M. A. Schmidt, in *Transducers' 01 Eurosensors XV*, Springer, Berlin **2001**, pp. 30–33.
- [133] X. Bai, J. Liu, *J. Eng. Thermophys.* **2005**, 26, 826.
- [134] C.-Y. Sue, N.-C. Tsai, *Appl. Energy* **2012**, 93, 390.
- [135] Y. Shi, Y. Wang, Y. Deng, H. Gao, Z. Lin, W. Zhu, H. Ye, *Energy Convers. Manage.* **2014**, 80, 110.
- [136] I. Stark, *Micro Energy Harvesting*, Wiley, New York **2015**, pp. 245–269.
- [137] S. Li, X. Wang, H. Xing, C. Shen, in *PowerMEMS Workshop*, IEEE, Freiburg, Germany, Vol. 2007, **2007**.
- [138] E. Ogbonnaya, A. Gunasekaran, L. Weiss, in *ASME 2011 Int. Mechanical Engineering Congress and Exposition*, American Society of Mechanical Engineers, New York **2011**.
- [139] E. Ogbonnaya, L. Weiss, in *Technical Proc. of the 38th Annual NSBE National Convention*, NSBE, Pittsburgh, PA, USA **2012**.
- [140] M. Mizoshiri, M. Mikami, K. Ozaki, K. Kobayashi, *J. Electron. Mater.* **2012**, 41, 1713.
- [141] D. M. Rowe, D. V. Morgan, J. H. Kiely, *Electron. Lett.* **1989**, 25, 166.
- [142] J. Weber, K. Potje-Kamloth, F. Haase, P. Detemple, F. Völklein, T. Doll, *Sens. Actuators, A* **2006**, 132, 325.
- [143] S. B. Inayat, K. R. Rader, M. M. Hussain, *Sci. Rep.* **2012**, 2, 841.
- [144] V. L. Koppa, S. M. Tangutooru, G. G. Nestorova, E. J. Guilbeau, *Sens. Actuators, B* **2012**, 166, 608.
- [145] N. Wojtas, E. Schwyter, W. Glatz, S. Kühne, W. Escher, C. Hierold, *Sens. Actuators, A* **2012**, 188, 389.
- [146] B. Mathew, B. Jakub-Wood, E. Ogbonnaya, L. Weiss, *Int. J. Heat Mass Transfer* **2013**, 58, 492.
- [147] M. Kishi, H. Nemoto, T. Hamao, M. Yamamoto, S. Sudou, M. Mandai, in *Eighteenth International Conference on Thermoelectrics*, IEEE, Piscataway, NJ **1999**.
- [148] Z. Wang, V. Leonov, P. Fiorini, C. Van Hoof, *Sens. Actuators, A* **2009**, 156, 95.
- [149] M.-K. Kim, M.-S. Kim, S. Lee, C. Kim, Y.-J. Kim, *Smart Mater. Struct.* **2014**, 23, 105002.
- [150] Q. Brogan, T. O'Connor, D. S. Ha, in *2014 IEEE Int. Symp. on Circuits and Systems (ISCAS)*, IEEE, Piscataway, NJ **2014**.
- [151] T. Torfs, V. Leonov, B. Gyselinckx, in *2006 5th IEEE Conf. on Sensors*, IEEE, Piscataway, NJ **2006**.
- [152] J. Lueke, W. A. Moussa, *Sensors* **2011**, 11, 1433.
- [153] E. J. Guilbeau, B. C. Towe, M. J. Muehlbauer, *ASAIO J.* **1987**, 33, 329.
- [154] Y. Yang, X.-J. Wei, J. Liu, *J. Phys. D: Appl. Phys.* **2007**, 40, 5790.
- [155] D.-e.-B. Wang, X.-P. Liao, T. Liu, *J. Microelectromech. Syst.* **2012**, 21, 121.
- [156] J. Iannacci, *Sens. Actuators, A* **2018**, 187.
- [157] Y. Huang, R. Doraiswami, M. Osterman, M. Pecht, in *2010 Proceedings 60th Electronic Components and Technology Conference (ECTC)*, IEEE, Piscataway, NJ **2010**.
- [158] M. Cansiz, D. Altinel, G. K. Kurt, *Energy* **2019**, 174(C), 292.
- [159] H. H. R. Sherazi, L. A. Grieco, G. Boggia, *Ad Hoc Netw.* **2018**, 71, 117.
- [160] N. Kaur, N. Sharma, N. Kumar, *Indian J. Sci. Technol.* **2018**, 11, 25.
- [161] H. Dai, Y. Lu, M. K. Law, S. W. Sin, U. S. Pan, R. P. Martins, in *2015 IEEE Int. Wireless Symp. (IWS 2015)*, IEEE, Piscataway, NJ **2015**.
- [162] S. Selvan, M. Zaman, R. Gobbi, H. Y. Wong, *J. Electrom. Waves Appl.* **2018**, 32, 2110.
- [163] Y. Huang, M. Osterman, M. Pecht, in *2012 IEEE 62nd Electronic Components and Technology Conf. (ECTC)*, IEEE, Piscataway, NJ **2012**.
- [164] H. J. Visser, R. J. M. Vullers, *Proc. IEEE* **2013**, 101, 1410.
- [165] B. Parida, S. Iniyar, R. Goic, *Renewable Sustainable Energy Rev.* **2011**, 15, 1625.
- [166] M. Dale, S. M. Benson, *Environ. Sci. Technol.* **2013**, 47, 3482.
- [167] Y. Liang, Z. Xu, J. Xia, S.-T. Tsai, Y. Wu, G. Li, C. Ray, L. Yu, *Adv. Mater.* **2010**, 22, E135.
- [168] E. Nuxoll, *Adv. Drug Delivery Rev.* **2013**, 65, 1611.
- [169] R. Bogue, *Sens. Rev.* **2013**, 33, 300.
- [170] Y. Yang, J. Liu, *Front. Energy* **2011**, 5, 270.
- [171] Z. Abidin, M. A. Alim, R. Saidur, M. R. Islam, W. Rashmi, S. Mekhilef, A. Wadi, *Renewable Sustainable Energy Rev.* **2013**, 26, 837.
- [172] E. Franklin, V. Everett, A. Blakers, K. Weber, *Adv. Optoelectron.* **2007**, 2007, 035383.
- [173] A. Blakers, K. Weber, V. Everett, *Chem. Aust.* **2005**, 72, 9.
- [174] J. L. Cruz-Campa, G. N. Nielson, M. Okandan, P. J. Resnick, C. A. Sánchez, V. P. Gupta, J. S. Nelson, in *2013 IEEE 39th Photovoltaic Specialists Conf. (PVSC)*, IEEE, Piscataway, NJ **2013**.
- [175] Z. Jia, Z. Yu, G. F. Burkhard, C. M. Hsu, S. T. Connor, Y. Xu, Q. Wang, *Nano Lett.* **2009**, 9, 279.
- [176] C. Sierra, A. J. Vázquez, *J. Mater. Sci.* **2005**, 40, 1339.
- [177] A. Blakers, M. Taouk, S. Narayanan, M. A. Green, Z. Jianhua, in *Conf. Record of the 2006 IEEE 4th World Conf. on Photovoltaic Energy Conversion*, IEEE, Piscataway, NJ **2006**.
- [178] E. Franklin, V. Everett, A. Blakers, K. Weber, in *Conf. Record of the 2006 IEEE 4th World Conf. on Photovoltaic Energy Conversion*, IEEE, Piscataway, NJ **2006**.
- [179] G. N. Nielson, W. V. Schoenfeld, J. J. Wang, M. Okandan, J. L. Cruz-Campa, M. Loncar, T. J. Suleski, P. J. Resnick, M. W. Wanlass, P. J. Clews, T. C. Pluym, in *Advanced Fabrication Technologies for Micro/Nano Optics and Photonics IV*, International Society for Optics and Photonics, xxxx **2011**.
- [180] J. L. Cruz-Campa, D. Zubia, X. Zhou, D. Ward, C. A. Sánchez, J. J. Chavez, B. A. Aguirre, F. Anwar, D. Marrufo, E. D. Spoerke, C. Chan, P. Lu, M. J. Rye, H. Prieto, J. C. McClure, G. N. Nielson, in *27th European Photovoltaic Solar Energy Conference*, The EEA, Frankfurt, Germany **2012**.
- [181] E. S. Mungam, C. Lu, V. Raghunathan, K. Roy, in *Proc. of the 2012 ACM/IEEE Int. Symp. on Low Power Electronics and Design*, ACM, xxxx **2012**.
- [182] V. Emelyanov, N. Kaluzhnyi, S. Mintairov, M. Shvarts, V. Lantratov, in *International Conference on Micro and Nano-Electronics 2009*, International Society for Optics and Photonics, xxxx **2010**.
- [183] F. Kessler, D. Rudmann, *Sol. Energy* **2004**, 77, 685.
- [184] M. A. Green, *J. Mater. Sci.: Mater. Electron.* **2007**, 18, 15.
- [185] W. Shockley, H. J. Queisser, *J. Appl. Phys.* **1961**, 32, 510.
- [186] B. O'regan, M. Grätzel, *Nature* **1991**, 353, 737.
- [187] M. Grätzel, *J. Photochem. Photobiol., C* **2003**, 4, 145.
- [188] J. Burschka, N. Pellet, S.-J. Moon, R. Humphry-Baker, P. Gao, M. K. Nazeeruddin, M. Grätzel, *Nature* **2013**, 499, 316.
- [189] Z. L. Wang, W. Wu, *Angew. Chem., Int. Ed.* **2012**, 51, 11700.
- [190] A. P. Alivisatos, *Science* **1996**, 271, 933.
- [191] D. J. Friedman, *Curr. Opin. Solid State Mater. Sci.* **2010**, 14, 131.
- [192] H. Cotal, C. Fetzer, J. Boisvert, G. Kinsey, R. King, P. Hebert, H. Yoon, N. Karam, *Energy Environ. Sci.* **2009**, 2, 174.
- [193] C. Kerestes, L. Wang, A. Gerger, A. Lochtefeld, R. Opila, A. Barnett, in *2011 37th IEEE Photovoltaic Specialists Conf. (PVSC)*, IEEE, Piscataway, NJ **2011**.
- [194] X. Sheng, C. A. Bower, S. Bonafede, J. W. Wilson, B. Fisher, M. Meitl, H. Yuen, S. Wang, L. Shen, A. R. Banks, C. J. Corcoran, R. G. Nuzzo, S. Burroughs, J. A. Rogers, *Nat. Mater.* **2014**, 13, 593.
- [195] J. Yoon, A. J. Baca, S. Park, P. Elvikis, J. B. Geddes, L. Li, R. H. Kim, J. Xiao, in *Materials for Sustainable Energy: A Collection of Peer-Reviewed Research and Review Articles from Nature Publishing Group*, World Scientific, Singapore **2011**, pp. 38–46.
- [196] A. Sacco, D. Pugliese, A. Lamberti, M. Castellino, A. Chiodoni, A. Virga, S. Bianco, *Mater. Chem. Phys.* **2015**, 161, 74.
- [197] X. Wei, H. Lee, S. Choi, *Sens. Actuators, B* **2016**, 228, 151.



- [198] L. Reshma, A. Chaitanyakumar, A. L. G. N. Aditya, B. Ramaraj, K. Santhakumar, *Algal Res.* **2017**, 26, 47.
- [199] V. Narasimhan, D. Jiang, S.-Y. Park, *Appl. Energy* **2016**, 162, 450.
- [200] J. M. Donelan, Q. Li, V. Naing, J. A. Hoffer, D. J. Weber, A. D. Kuo, *Science* **2008**, 319, 807.
- [201] J. Rosen, J. Perry, N. Manning, S. Burns, B. Hannaford, in *12th Int. Conf. on Advanced Robotics, 2005 (ICAR'05) Proc.*, IEEE, Piscataway, NJ **2005**.
- [202] A. C. R. Grayson, R. S. Shawgo, A. M. Johnson, N. T. Flynn, Y. Li, M. J. Cima, R. Langer, *Proc. IEEE* **2004**, 92, 6.
- [203] S. Cheng, Z. Wu, *Lab Chip* **2012**, 12, 2782.
- [204] S.-Y. Wu, W. Hsu, *Lab Chip* **2014**, 14, 3101.
- [205] A. W. Martinez, S. T. Phillips, Z. Nie, C.-M. Cheng, E. Carrilho, B. J. Wiley, G. M. Whitesides, *Lab Chip* **2010**, 10, 2499.
- [206] L. T. Wagner, J. Yang, S. Ghobadian, R. Montazami, N. Hashemi, *Open J. Appl. Biosens.* **2012**, 1, 21.
- [207] J. S. Ho, A. J. Yeh, E. Neofytou, S. Kim, Y. Tanabe, B. Patlolla, R. E. Beygui, A. S. Y. Poon, *Proc. Natl. Acad. Sci. USA* **2014**, 111, 7974.
- [208] G. Chen, X. Liu, S. Li, M. Dong, D. Jiang, *Lab Chip* **2018**, 18, 1026.



**M. A. Parvez Mahmud** received his B.Sc. degree in Electrical and Electronic Engineering and Master of Engineering degree in Mechatronics Engineering. After the successful completion of his Ph.D. degree with multiple awards, he worked as a Postdoctoral Research Associate and Academic in the School of Engineering at Macquarie University, Sydney. He is currently an Alfred Deakin Postdoctoral Research Fellow at Deakin University, Melbourne. His research interest includes piezoelectric and triboelectric energy harvesters, toward the development of self-powered flexible electronic devices.



**Sajad Razavi Bazaz** received his M.Sc. degree as a first rank student in biomedical engineering from University of Tehran, Iran, in 2017. He currently holds a position as a Ph.D. candidate in School of Biomedical Engineering at University of Technology Sydney. His main research interest is to investigate fundamentals of inertial microfluidics in rigid microchannels and design and fabricate functional 3D printed inertial microfluidic devices for particle/cell separation, bioprocessing industry, and intracellular delivery.



**Mohsen Asadnia** is a senior lecturer, ARC DECRA fellow and group leader at the School of Engineering, Macquarie University. He received his Ph.D. in Mechanical Engineering from Nanyang Technological University (NTU)-Singapore. He undertook his postdoctoral training at Massachusetts Institute of Technology (SMART center) and the University of Western Australia (UWA). He has been a group leader at Macquarie University since 2016. His research interests are ion selective membranes, chemical sensors, MEMS/ NEMS bio-inspired sensory systems, biomimetic devices, artificial hair cells of the vertebrate inner ear and microfluidic devices.



**Majid Ebrahimi Warkiani** is a Professor in Biomedical Engineering at University of Technology Sydney. He completed his Ph.D. program at Nanyang Technological University and subsequently undertook postdoctoral training at Singapore–MIT Alliance for Research and Technology (SMART) center. He is NHMRC-CD fellow and also a member of Institute for Biomedical Materials & Devices (IBMD) and Center for Health Technologies (CHT) at UTS. Dr Warkiani's current research activities focus on three key areas of a) microfluidics, b) organ-on-a-chips, and c) 3D printing.



**Zhong Lin Wang** is the Hightower Chair in Materials Science and Engineering, Regents' Professor, Engineering Distinguished Professor at GeorgiaTech. He is a foreign member of the Chinese Academy of Sciences, fellow of American Physical Society, fellow of AAAS, fellow of Microscopy Society of America, and fellow of Materials Research Society. He has been awarded the MRS Medal and Burton Medal. His discovery in nanogenerators establishes the principle and technological roadmap for harvesting mechanical energy from environment. His most important contributions in science are: pioneered the field of nanogenerators and self-powered sensors; coined piezotronics and piezophototronics for the third-generation semiconductors.